FINAL REPORT

REDUCED GRAVITY BATTERY TEST PROGRAM

Research and Development Center
General Electric Company
Schenectady, New York

Contract Number: 952121

March 1969

Prepared for:

Jet Propulsion Laboratory
California Institute of Technology
Pasadena, California 91109

S-69-1081

Final Report

REDUCED GRAVITY BATTERY TEST PROGRAM

Research and Development Center
General Electric Company
Schenectady, New York

Contract Number: 952121

March 1969

This work was performed for the Jet Propulsion Laboratory, California Institute of Technology, as sponsored by the National Aeronautics and Space Administration under Contract NAS 7-100

FOREWORD

This report was prepared by the General Electric Company, Schenectady, New York, on J.P.L. Contract Number 952121. This contract is a subcontract under NASA Contract NAS 7-100, Task Order No. RD-26. This contract is administered by the Jet Propulsion Laboratory, California Institute of Technology, Pasadena, California. Mr. G.L. Juvinall is the designated JPL Technical Representative for the Laboratory.

The work presented in this Final Report was accomplished between August 20, 1968 and February 20, 1969. The work was performed by the Research and Development Center of the General Electric Company.

Principal contributors were: A.J. Yerman, Technical Director; Dr. W.J. van der Grinten, Senior Chemical Physicist; J.M. Holeman, Engineer--Optical Systems; S.C. Richardson, Engineer--Measurements and Instrumentation; M.D. Ketchum, Engineer--Electronic Systems; and E. Siwek, Specialist--Battery Technology.

ABSTRACT

This is the final report of JPL Contract No. 952121 with the General Electric Company Research and Development Center covering the design, construction and testing of a Breadboard Unit capable of investigating the behavior of secondary Ag-Zn batteries in the zero-g environment of an earth orbit. Three types of test are to be performed automatically in sequence by the equipment.

This report covers the test results obtained from the Breadboard Unit as implemented. These tests verified the adequacy of the solid state logic test programming approach used, the data acquisition methods employed, and established that average power levels for the complete equipment were within the target specification.

Tests of two of the experiments (Task 1 and Task 3) yielded highly repeatable results which closely checked previous measurements. Task 1 tests of plain zinc electrodes showed a 55% reduction of limiting current density under simulated zero-g conditions. Task 3 tests of commercial quality Ag-Zn cells showed surprisingly little loss in discharge capacity until after 10 stress cycles to 100% depth of discharge. Beyond this point degradation of cell characteristics proceeded rapidly.

Results of tests of the Task 2 experiment did not agree with earlier bench top experiments. Some of the differences noted have been attributed to differences in electrode construction, and some to deficiencies in the gas management system employed. An outline of additional work required to eliminate difficulties encountered in the Task 2 experiment is presented.

SUMMARY

This is the final report of JPL Contract No. 952121 with the General Electric Company Research and Development Center covering the design, construction and testing of a Breadboard Unit of equipment for investigating the behavior of Ag-Zn secondary batteries in the zero-g environment of an earth orbit. Three types of test are performed by the equipment in an automatic sequence. In the first test, a group of six special cells with smooth zinc electrodes are activated and the limiting current density (LCD), of each is measured using a linear current-ramp loading technique. This test is designed to measure changes in battery performance due to gravity sensitive convective transport processes. In the second test, two special batteries designed to permit photographic observation of bubble behavior at the electrode-separator interface, are employed as a test device to measure effects of gas bubbles on the discharge capacity of porous commercial zinc and silver electrodes. The third test is designed to measure any degradation in discharge cycle life of six 5 AH commercial silver-zinc batteries when subjected to zero-gravity.

The objectives of the program included establishment of detailed test objectives, design of test equipment and instrumentation for implementing the tests, construction of a "Breadboard Model" of the test equipment and instrumentation system, and carrying out a suitable test program to evaluate the system performance.

Approximately 750 hrs. of trouble-free operation during the test program has indicated that the solid state logic and control system employed in the three experiments was a reliable and trouble free approach. It proved to be insensitive to expected supply voltage and temperature

variations and maintained system power consumption within the limits set by the initial contract definition. During tests, all electrical measurements were recorded on magnetic tape at a very low tape speed (0.06 ips). In the third test which required recording times of 6 to 8 days, tape efficiency was further improved by recording on a sampled data basis for 14 sec. every 72 sec. with the tape transport arrested when not recording. Playback of these tapes at 1 7/8 ips has the advantage of time compression and showed negligible loss of accuracy in both sampled and continuous records.

Test results from experiments 1 and 3 were found to be highly repeatable and closely checked previous experimental work. The plain zinc electrodes of experiment 1 showed a 55% reduction in LCD under zero-g conditions simulated by orienting the cells so that convection was suppressed. The commercial quality batteries employed in the third experiment proved to be more durable at high depth-of-discharge than original estimates indicated. Little degradation was noted until after 10 stress cycles to 100% depth of discharge. This means that it may be necessary to modify the test program employed there to achieve a significant level of degradation within the test time period. Flexibility built into the Breadboard Unit should permit the additional test data acquisition necessary to define a modified test program.

The results obtained in tests of the equipment for experiment 2 did not agree with results from earlier bench top experiments. In general the amount of additional discharge capacity resulting from removal of gas from the electrode was much less than previous tests had indicated. The differences noted have been attributed to differences in electrode

construction and deficiencies in the gas management system employed. Several methods of improving the gas handling system are recommended for further test and development along with changes in electrode design and test procedures intended to accentuate gas effects at the electrode surface.

The results of this test program indicate the general adequacy of the equipment design and experimental approach with exceptions as noted in the case of the second experiment. Also, the results of tests conducted on commercial batteries in experiment 3 tend to point up the inadequacy of currently available information on Ag-Zn battery performance as a basis for the design of power supplies in many deep space experiments. We are referring, not just to a lack of information on effects of weightlessness, the acquisition of which is the thrust of this program, but to deficiencies in essential information regarding performance characteristics such as depth-of-discharge on the cycle life of batteries. The lack of such detailed information requires the use of large safety factors in system designs with an attendant decrease in payload efficiency.

Since such information can be readily obtained with the Breadboard Unit on a semiautomatic basis by varying certain test parameters, the equipment developed under this program should prove to be a useful experimental tool for laboratory investigations of battery characteristics, as well as serving as the test bed for proving out techniques usable in testing gravity dependent effects on batteries.

TABLE OF CONTENTS

TABLE OF CONTENTS

LIST OF FIGURES

LIST OF FIGURES

LIST OF TABLES

REDUCED GRAVITY BATTERY TEST PROGRAM

1.0 INTRODUCTION

Prior work by Jet Propulsion Laboratory, California Institute of Technology on smooth zinc electrodes and alkaline electrolytes has shown that gravity has significant effects on electrode performance with wide variations in the effect resulting when the internal geometry of the cell is changed. Extrapolation of these results at one gravity and higher to 0 gravity conditions is revealing, but uncertainties in this procedure detract from the usefulness of such results. Also there are questions regarding the validity of applying such test results to commercial silver zinc batteries where electrode spacings are minimal, and any convection effect would be greatly suppressed. However, in view of the magnitude of the effects noted, it is essential that more detailed information be acquired on low g effects by direct measurement. Because of the wide spread use of silver zinc batteries in space programs, recognition of this need has resulted in the Jet Propulsion Laboratories sponsorship of a R&D program under contract number 952121. Under this contract starting February 21, 1968, the General Electric Research and Development Center undertook a program which had the objectives of carrying out background research, formulating test procedures, and finally designing, fabricating, and testing a Breadboard Unit of a test system which would be capable of investigating the behavior of Ag-Zn batteries during flight in a low or 0-g environment.

The Breadboard Unit is to be capable of conducting 3 separate tests, which have been designated with task numbers as follows:

Task 1 - To measure the limiting current density of a smooth pure zinc anode in the region of 0 to 1-g, in an experiment designed to

provide maximum correlation with data previously obtained by JPL over a 1 to 20-g range.

Task 2 - To investigate the performance of battery electrodes in special silver zinc research cells as a function of bubble formation on the electrode surface.

Task 3 - To measure the electrical capacity of a secondary silver zinc cell as a function of charge discharge cycling in a 0 to 1-g environment as well as the limiting current capability (polarization curve).

During the first quarter of the contract, effort was concentrated mostly on Tasks 1 and 3. Considerable experimental work was carried out in an effort to better define these individual experiments, and provide information for the design of an adequate test control and instrumentation system. The results obtained are covered in the First Quarterly Report.[1] During the second quarter[2], the basic experimental work necessary to define the test procedures and equipment requirements of the Task 2 experiment were carried out. This involves the photographic observation of gas bubble formation and distribution on the electrodes of specially designed silver zinc secondary batteries during charge and discharge cycles.

As a result of this experimental work, test concepts were formulated and an equipment design study was carried out which resulted in a proposal for implementation of the three experiments. Test procedure and equipment proposals were documented in an additional report[3] issued in July 1968

(1) Quarterly Report No. 1, "Reduced Gravity Battery Test Program" contract No. 952121, General Electric R&D Center, Report S-68-1087, July 1968.

(2) Quarterly Report No. 2, "Reduced Gravity Battery Test Program" contract No. 952121, General Electric R&D Center, Report S-68-1140, September 1968.

(3) Test Plan and Test Procedures for Reduced Battery Test Program contract 952121, General Electric R&D Center, Report S-68-1118, July 1968.

which recommended a design, operating procedures, and functional tests for the Breadboard Unit to be fabricated, tested, and delivered to JPL as part of the Reduced Gravity Battery Test Program. The Breadboard Unit design is intended to be a realistic model of similar equipment which will be eventually flown in a space experiment. Thus, its design and components were selected insofar as possible so that a minimal amount of change would be required when the flight unit was designed. Following approval of the test plan, the R&D Center fabricated the Breadboard Unit and carried out a testing program to evaluate it. The results of that test program are the primary subject of this final report.

Where changes have been made in either test procedures or equipment design from those proposed in the test plan, they are fully discussed in this report. However, not included here is detailed information on the hardware and maintenance aspects of the equipment. That is covered in a separate document which is being issued concurrently.[4] This report has separate sections devoted to each of the three experiments carried out by the equipment. Each section contains a brief description of the experiment and test sequence, together with test results obtained. Where possible these are compared to prior results reported earlier in the program.

Additional sections cover measured power consumption during operation of the equipment and from this and other information weight and power for a flight model of this equipment are projected. A final section presents conclusions drawn from the experimental results and recommendations for future activity. Figure 1.1 shows the complete Breadboard Unit.

(4) Instruction Book, GEI 45092 Reduced Gravity Battery Test Equipment, General Electric Company Research and Development Center, March 1969

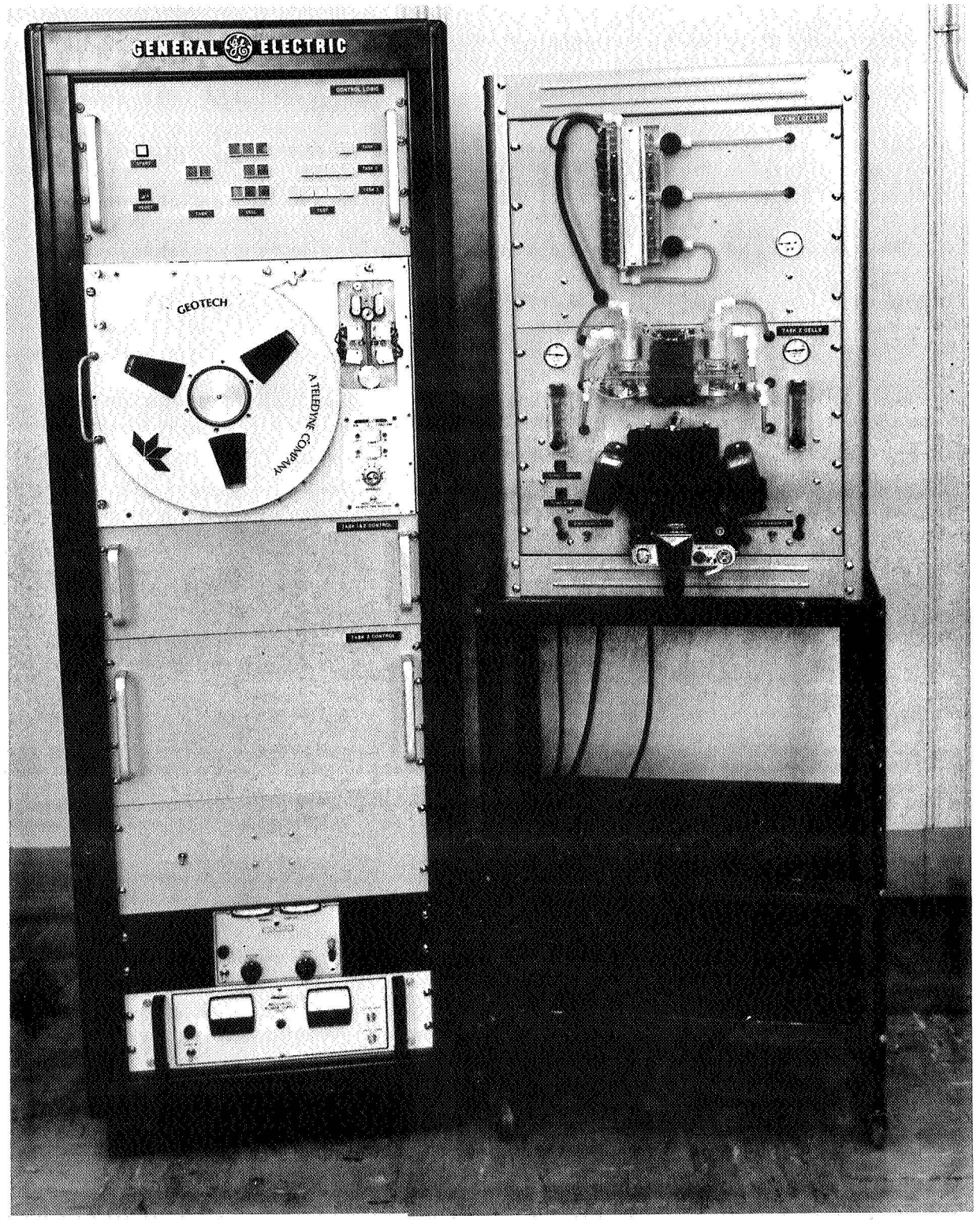

Figure 1.1. Complete Breadboard Unit, Reduced Gravity Test Equipment

2.0 TASK 1 - EXPERIMENT

2.1 Introduction

The Task 1 experiment may be viewed as primarily an automated implementation of experiments originally carried out by Jet Propulsion Laboratory on smooth zinc electrodes. However, there are some significant deviations from the original test procedure.(5)

In the original work, the limiting current density of a one square centimeter area of smooth zinc electrode was determined by loading the cell with successfully larger discharge currents with each level maintained constant for a time interval of 1 minute. This "staircase type" of current-time loading function was terminated when the voltage between the zinc and the zinc reference electrode dropped to a value of 1 volt. The maximum current level reached just prior to polarization was defined as the limiting current density.

In the interest of improving repeatability of this type of test we substituted a linear current-time ramp type of loading. Earlier tests had shown that this type of loading gave very repeatable results, which could be correlated to the test results JPL had obtained previously. Since implementation of this experimental approach was much less complicated than the former, it was incorporated into the equipment design.

As explained in Quarterly Report No. 1, Section 1.1, the LCD determining transport process is gravity dependent if the zinc electrode is placed in the vertical position. In the horizontal position, on the other hand, such processes normally are not gravity dependent so that the horizontally

(5) JPL Space Program Summaries, Volume 5, pages 73-23, 73-26, and 73-30 (1966).

oriented zinc electrode at the bottom, and at 1-g, can be looked upon at least qualitatively as a "simulation" of the 0-g environment. However, it was found desirable in carrying out such tests, to maintain a reasonably well balanced depth-of-discharge (DOD) in order to maintain an equivalent degree of etching of the polished zinc electrode and similar specific gravity changes of the electrolyte regardless of orientation. This could be most readily accomplished by using different current ramp slopes corresponding to the two different electrode orientations.

These considerations have been factored into the design of the breadboard model. As implemented, six identical cells are tested sequentially using a linear current ramp to determine the limiting current density of each cell. Provision is made so that the orientation of the cell electrode can be selected as either horizontal or vertical, and the slope of the current ramp is adjusted to suit the orientation selected by means of plug-in components. Thus the equipment provides an arrangement whereby tests similar to the original JPL tests can be carried out (gravity sensitive vertical electrode orientation) or 0 gravity can be simulated (horizontal electrode position).

2.2 Activation and Test Sequence

This experiment would ordinarily be carried out in two steps. In step number 1 the group of six test cells would be activated by introducing the electrolyte solution. This would be a manual operation by the astronaut. Once activated the automatic test sequence would be initiated by the astronaut. Once started, each of the six cells would be tested, and at the conclusion of the Task 1 experiment, the Task 2 experiment would be started automatically.

The discreet steps in these two parts of the Task 1 experiment are listed in Table 2-1.

The measurements made during the Task 1 experiment are defined in Table 2-2.

2.3 Description of Equipment

The test cell employed in this experiment is shown in Figure 2.1. This shows two of the Task 1 cells, one of which is assembled and the other disassembled. The cell case itself and the cover plate are fabricated from acrylic plastic. The auxiliary electrode employed in the cell case is a silver electrode taken from a Yardney HR5 type silver-zinc battery. The one square centimeter electrode area is defined on the zinc test electrode by means of an acrylic plastic mask. When the cell is assembled, an O-ring seal is used between the zinc test electrode and the main body of the cell. Contact with the zinc electrode is made by means of a silver wire welded to the backside of this electrode area. Connections to the silver electrode and a zinc reference electrode in front of it are brought out through the main body of the cell and sealed with a solution of acrylic plastic in dichloroethylene at the outer surface.

Each cell is provided with a stem electrolyte port through which the cell is filled when it is inserted in the manifold. The seal to the manifold system is accomplished by means of another O-ring on the stem of the cell. Electrolyte from the manifold enters the cell through a nylon capillary tube which provides a high electrical resistance path between cell and manifold. This is necessary in order to provide adequate electrical isolation between the cells when they are inserted in the manifold. This capillary has a bore diameter of about 40 mils and is approximately 6 inches long. This

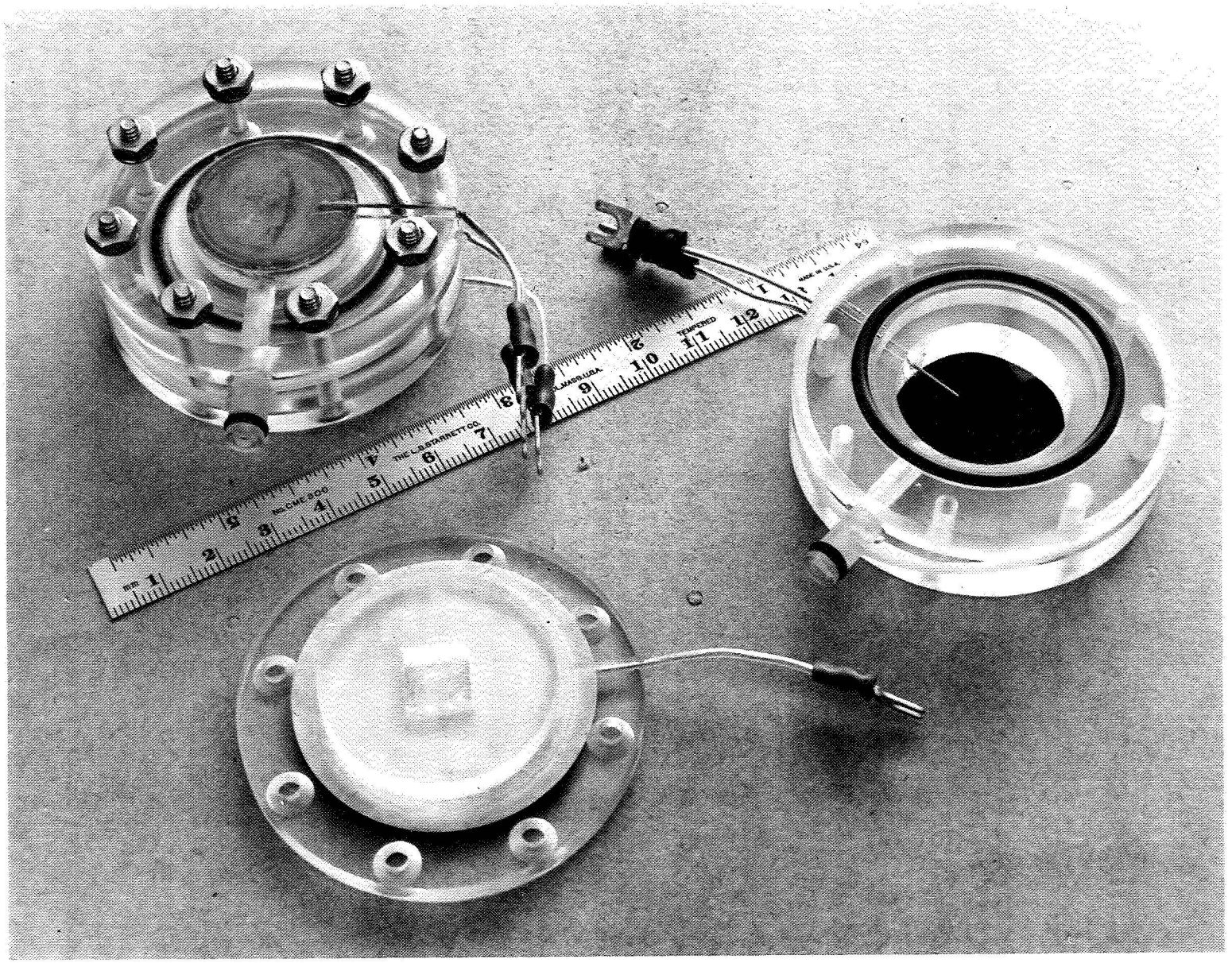

Figure 2.1. Task 1 Cell Assembly

TABLE 2-1

TASK 1 ACTIVATION AND TEST SEQUENCE DESCRIPTION

I. Activation of Task 1 Cells (preliminary manual operations by astronaut):

1. Open valve to evacuate Task 1 test cells
2. Close vacuum valve
3. Open valve to KOH reservoir to fill cells
4. Close fill valve
5. Vent cells to ambient

II. Task 1 Test Sequence (automatic, see note 6 following Table 2-2)
(see Table 2-2 for listing of measurements)

1. Calibration Sequence:
   a. Disconnect tape recorder measurement system
   b. Zero check of measurement channels 1-4
   c. Sensitivity check measurement channels
   d. Repeat Step b
   e. Repeat Step c
   f. Reconnect measurement system
2. Connect Battery Sample #1
3. L.C.D. Measurement Sequence:
   a. Start discharge current ramp (slope = 7 ma/min - see note 1, 2, Table 2-2)
   b. When maximum discharge current is reached (175 ma or see note 1) start calibration sequence (1a - 1f above)
4. Disconnect Battery Sample #1, connect Sample #2
5. Repeat L.C.D. Measurement Sequence (step 3)
6. & 7. Repeat Steps 4, 5 for Sample #3
8. & 9. Repeat Steps 4, 5 for Sample #4
10. & 11. Repeat Steps 4, 5 for Sample #5
12. & 13. Repeat Steps 4, 5 for Sample #6
14. Disconnect Battery Sample #6
15. Generate end-of-test signal

TABLE 2-2

TASK I MEASUREMENTS

Measurands	Recorder Channel	Measured Range	Resolution	Accuracy	Voltage Signal Available Volts (max)	Minimum Input Impedance Ohms	Sampling Rate Meas'ts/Min.	Test Time per Sample
Voltage: Zn Electrode to Zn ref.	1	0-1.2V	20 MV	±50 MV	1.2V	10K	Continuous	~15 min (Note 3)
Voltage: Cell	2	1.0-2.2V	20 MV	±50 MV	2.2V	10K		
Cell Current (ma)	3	0-100 (note 4)	2 MA	±5 MA	.065	10K		
Temperature (note 5)	4	0-50°C	0.1°C	1°C	.065	10K		
Elapsed Time	5	0-30 min.	1 sec	5 sec	←ref.freq.→ of tape recorder			

NOTES:

1. Ramp slopes to be determined by accessible components which can be readily changed to get other ramp slopes. Components will also be provided for 50 ma/min. slope with a maximum current of 250 ma.

2. Task 1 control system to have a timed override which generates an end-of-test signal after 3 hrs. which will initiate Task 2 sequence. This is to guard against cell failure or current ramp generator failure.

3. Based on zero g or zero g simulation with horizontal electrode. Test at low current range slope (7 ma/min) with vertical electrode at 1g will require up to 25 min. per sample.

4. Can be changed with replaceable resistor to 0 to 250 ma range.

5. One temperature sensor to measure average ambient temperature near six sample cells.

6. Six cells can be tested automatically under the following preselected conditions:

   a. horizontal electrode orientation
   b. vertical electrode orientation
   c. current ramp slope selected from options stated in note 1.

provides a resistance of about 10 Kilohms between cells via the electrolyte present in the common manifold. This resistance level is adequate to reduce leakage current between cells to negligible levels. A group of six of these cells is plugged into the test manifold used for activation. A terminal strip on the manifold provides connection of the three electrode leads from each cell. A photograph of the manifold with six cells inserted is shown in Figure 2.2.

At the conclusion of the Task 1 tests the cells and manifold remain in a vented condition. To prevent carryover of the electrolyte due to gas formation on standing over a period of time, a vent trap is provided as an integral part of the manifold. This consists of two rolled sections of 200 mesh nylon screen inserted in series in a 3/4" diameter hole through which vented gasses are conducted to the vent system. Since the nylon screen is readily wetted by the electrolyte it tends to be trapped in this screen while gas passes readily and a gas pressure buildup is prevented.

On Task 1 control panel shown in photograph 2.2, in addition to the cells and test manifold a small vacuum gage is provided to permit monitoring of manifold and cell pressure during the evacuation step prior to filling. Behind the panel, the electrolyte reservoir is mounted. It consists of an 8 ounce polyethylene bottle with sufficiently thin walls so that it tends to collapse under partial vacuum. When the electrolyte valve on the manifold is opened, this forces electrolyte into the evacuated cells.

2.4 Activation Procedures

Preliminary to the tests, a solution of zinc oxide saturated potassium hydroxide electrolyte is prepared. This consists of a 40% by weight solution

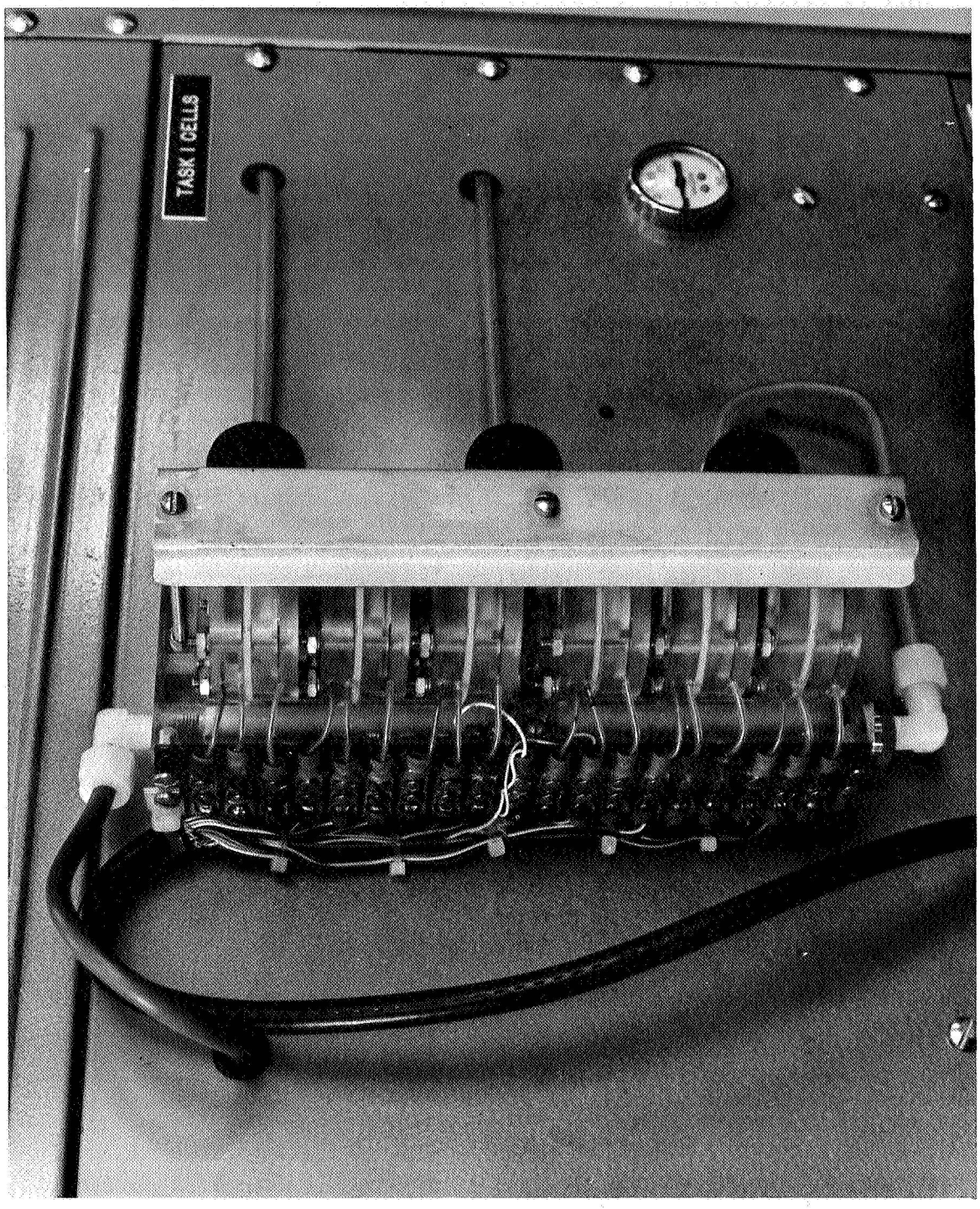

Figure 2.2. Task 1 Test Panel Showing Cell-Manifold Assembly

of KOH which is saturated with zinc oxide by stirring with surplus of zinc oxide present over a period of 2 days at room temperature. This mixture is then vacuum filtered and thoroughly degassed before transfer into the electrolyte reservoir.

2.5 Test Results

The Task 1 test has been carried out twice. In the first test the six test cells were oriented with the zinc electrode horizontal which simulates zero gravity conditions. A sample of the chart record taken during the course of this test is shown in Figure 2.3. The test record displays the 4 parameters measured which were, from top to bottom, zinc to zinc reference voltage, cell voltage, cell current, and ambient temperature.

In this test, which called for a nominal current ramp slope of 7 milliamps per minute, the actual slope was measured as 6.83 milliamps per minute. Two minor difficulties occurred during this test. The reference electrode on the first test sample opened so that zinc to zinc reference voltage measurements were not available for this cell. Also some overheating was noted in the IC amplifier controlling cell current at current levels beyond those which caused full polarization of the cell. This defect was corrected in subsequent tests and is discussed in Section 2.5.3 below. Neither of these difficulties caused the loss of any significant data.

Table 2-3 summarizes the results of the Task 1 test on horizontal electrode samples. The consistency of the results in cell to cell tests is quite evident. The second test of Task 1 was carried out with the cell electrodes oriented in the vertical position. Figure 2.4 is a sample of the results obtained on cell No. 4 in this test.

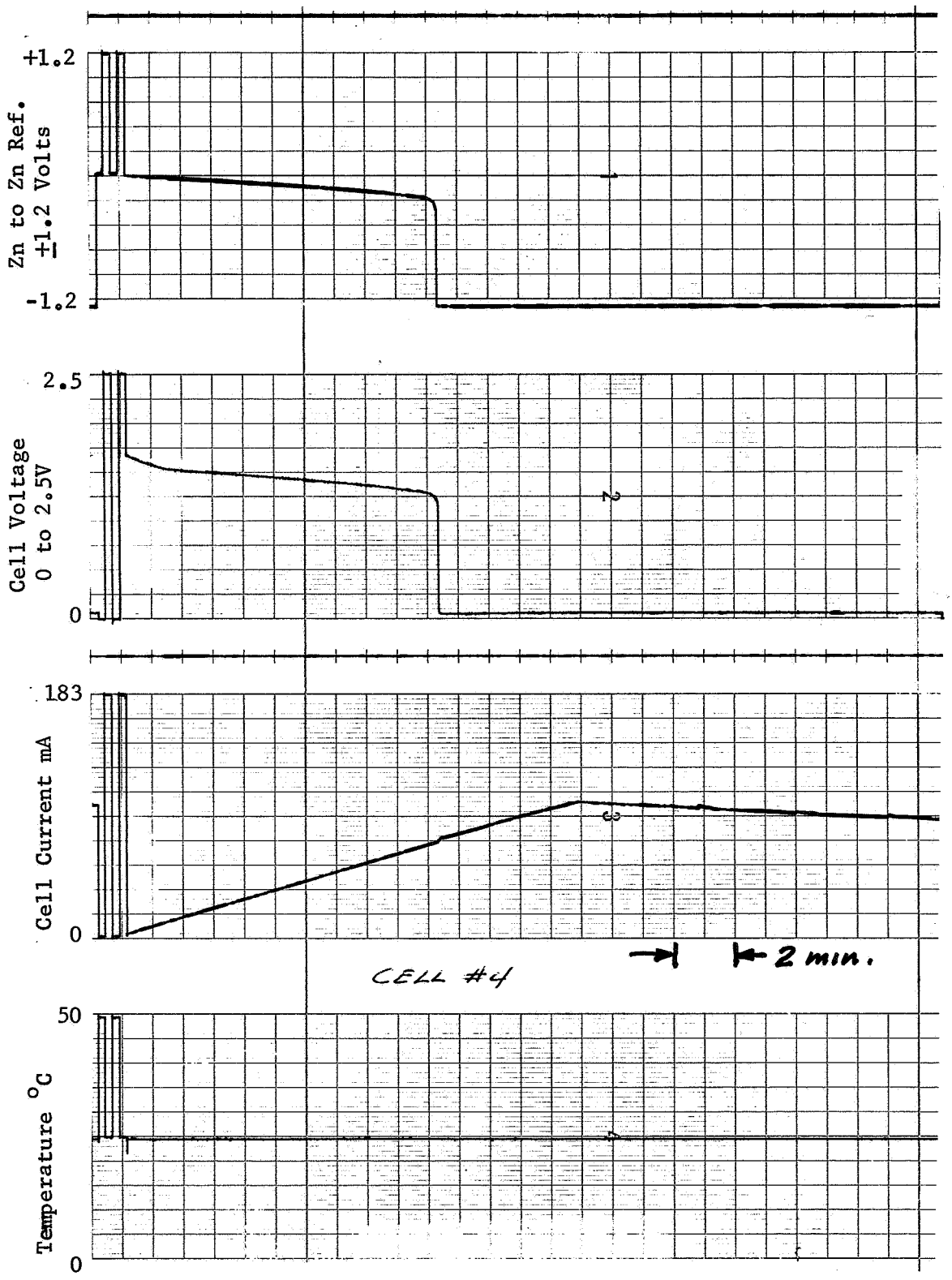

Figure 2.3

Task 1 Record Cell #4 Horizontal Orientation

TABLE 2-3

Results of Task 1 Test - Horizontal Electrode Position

Current Ramp Slope: 6.83 ma/min

Temperature: 24.5°C

Test Cell No.	LCD ma/cm^2	Time To Polarization Min.	Discharge Cap. ma-min
1	65.8	9.3	295
2	65.8	9.3	295
3	69.5	10.1	342
4	69.5	10.2	354
5	65.8	9.5	306
6	65.8	9.7	320
MEAN:	67.03	9.68	318.7

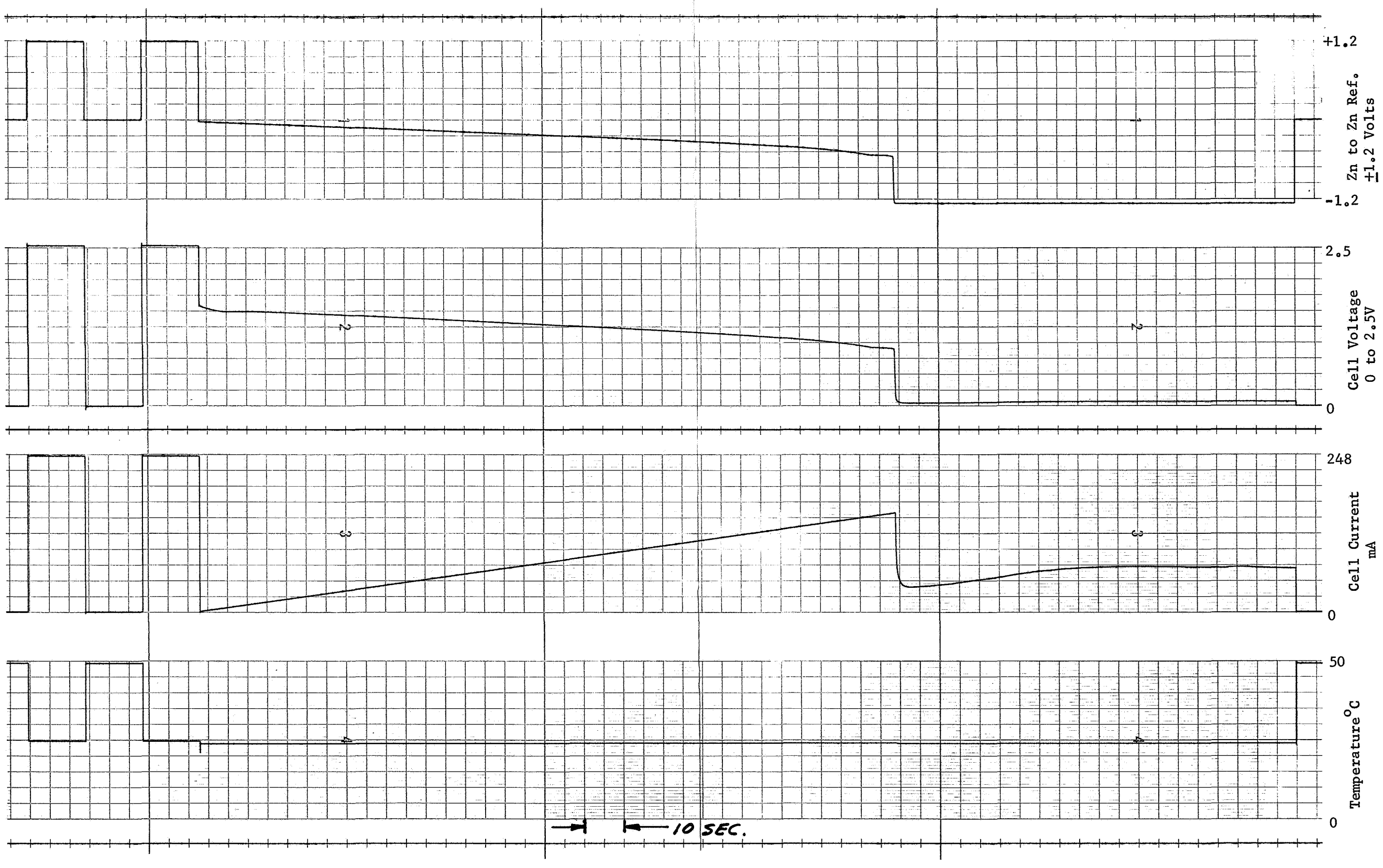

Figure 2.4. Sample Chart Record, Task 1 Test, Vertical Electrode

Prior to this test the difficulty mentioned previously was remedied. This accounts for the somewhat different curve shape on the cell discharge current in this test. The results of this test are summarized in Table 2-4.

2.5.3 Circuit Performance

The overall circuit performance of the Task 1 system has been good. The ramp rates are stable and quite linear over the range of operation.

One problem that arose early in the testing program was excessive heating of the μA709 amplifier in the current control circuit. The μA709 overheated after the Task 1 cells had polarized and the cell voltage had dropped to zero. When the cell voltage is zero, the driving transistor (2N3054) looks like a forward biased diode to the output of the μA709. The forward biased diode is essentially a short circuit on the output of the μA709 and caused the amplifier to overheat. The circuit has been modified by the addition of a second driving transistor (in a Darlington configuration) and a current limiting resistor. With this modification, the cell voltage can remain zero indefinitely without damage to the μA709.

2.6 Discussion of Test Results

Although the internal consistency of the test results obtained on the 6 cells and reported in the previous section is quite remarkable, all values obtained, including the vertical to horizontal LCD-ratios, are distinctly lower than those obtained earlier on individual bench-top cells. See Table 1-2, Ref. (2). A substantial number of seemingly unimportant changes have been incorporated into the test procedure since the bench-top tests were made. Obviously one or more of these must be responsible for this discrepancy, but it is impossible at this time to pinpoint any of those.

TABLE 2-4

Results of Task 1 Test - Vertical Electrode Position

Current Ramp Slope: 52.8 ma/min

Temperature: 24°C

Test Cell No.	LCD ma/cm^2	Time To Polarization Min.	Discharge Cap. ma-min
1	141.4	2.68	190
2	139.0	2.60	179
3	149.0	2.80	207
4	156.2	2.93	227
5	141.3	2.68	190
6	151.3	2.85	215
MEAN:	146.37	2.757	201.3

Nevertheless, the position dependence of the LCD's is as obvious as ever, suggesting a strong gravity dependence in the 0 - 1 region.

Matching the discharge capacities can be further improved by bringing the two current ramp slopes somewhat closer together.

3.0 TASK II EXPERIMENT

3.1 Introduction

The objective for this task is to investigate the performance of porous silver zinc battery electrodes as a function of the photographically recorded presence or absence of gas bubbles on the electrode surfaces. The experiment consists of measurements of the electrical capacity of a special design of research cell during a cycle designed to induce bubble formation, together with a photographic record of the physical behavior of the bubbles and the gas-liquid phase distribution within the cell. The overall objective is to compare such behavior in a 0-g environment with behavior ordinarily encountered at 1-g.

The initial work on this task is covered in the Second Quarterly Report[2]. There, a test procedure was described which compared the discharge capacity of a gas covered electrode with one which was gas free. In that test procedure, a partial discharge capacity (D1) of a fully charged and gas loaded test electrode measured under high constant current density conditions was compared to the residual discharge capacity (D2) of the same electrode after the gas cover had been removed. The effect of trapped gas on capacity was then measured as the ratio of D2 to D1. If the trapped gas had no effect, this ratio would approach 0, which was found to be the case for very low current densities. In contrast, for current densities in the range of 50 to 100 mA/cm^2 on zinc electrodes from a Yardney HR5 cell, D2/D1 values in excess of 1.1 were obtained. All of the initial tests were made with an open cell bench top set up which permitted observation of the test electrode surface through a microscope while the test was being conducted.

Out of this work a special cell was designed which permitted photographs

to be taken of the test electrode during the course of the experiment. This closed cell had provision for the removal of the gas cover on the electrode by means of an evacuation cycle, and additionally, it included a gas separator which was to be used in conjunction with a re-circulating pump to control gas distribution in the cell. One of these special cells was bench tested with recirculated electrolyte and a zinc test electrode. The results were found to be comparable to the earlier work with the open bench top cell. Based on these initial results a proposal for implementing this test was made in the Test Plan.[3] In general that approach has been followed in fabricating the breadboard equipment.

Consequently, two of these cells were fabricated, one which would permit testing the zinc electrode and second the silver electrode. The final breadboard implementation of these provided the equipment for taking the photographs, control switching for carrying out the test sequence, and the necessary pumps and plumbing for recirculating the electrolyte and separating gas. Some minor deviations from recommendations of the Test Plan have seemed advisable during the construction phase. Where this has occurred, they are described in detail in the following sections. This section of the report is devoted primarily to: (1) A description of the Task II experiment as implemented in the breadboard model; (2) The results obtained from tests carried out with the breadboard model.

3.2 Activation and Test Sequences

For reference purposes the activation and test sequence as proposed in the Test Plan is included below as Table 3-1. Associated with this is Table 3-2 which lists the measured parameters for the Task II experiment. Reference will be made to these two tables in the discussion below where changes have been found to be necessary.

TABLE 3-1

TASK 2 ACTIVATION AND TEST SEQUENCE DESCRIPTION

I. Activation of Task 2 Cells (Preliminary manual operation by astronaut to follow immediately after steps 1 - 5 of part I of Table 2-1)

1. Switch on two valves to evacuate the two test cells (zinc and silver electrodes).

2. Turn both circulating pumps on.

3. Open manually two reservoir valves to fill two test systems with metered volume of KOH electrolyte.

4. Close fill valves.

5. Switch off vacuum valves.

6. Open two backfill valves.

7. Close two backfill valves.

II. Task 2 Test Sequence (automatic) (see note 5 following Table 3-2)

A. Zinc Test Cell

1. Calibration Sequence (see Table 2-1 part II steps 1a thru 1f).

2. Connect zinc test cell.

3. Photograph zinc electrode, start cell charge at an initial current of 6 ma. (note 1)

4. Photo, stop cell charge when V_r = -0.25 volt (note 6) (charge time $\sim$ 1/2 hr.)

5. Photo, start discharge at $\sim$ 20 ma to determine D_1. (see note 2)

6. Photo, terminate discharge when V_r = +0.50 volt (discharge time < 1 hr.)

7. Photo, connect cell to vacuum for 1 min.

8. Photo, shut-off vacuum, and backfill to ambient for 1 min.

9. Photo, connect cell to vacuum for 1 min.

10. Photo, shut-off vacuum and backfill to ambient for 1 min.

11. Photo, start discharge at $\sim$ 20 ma to determine D_2. (see note 3)

TABLE 3-1 (continued)

12. Photo, terminate discharge when V_r = +0.50 volt (discharge time < 1 hr.)

13. Photo, generate end of test signal.

B. Silver Test Cell

1. Calibration Sequence (see Table 2-1, Part II, Steps 1a thru 1f).

2. Disconnect zinc cell, connect silver cell.

3. Photo, start charge at an initial current of 12 ma. (see note 1)

4. Photo, terminate charge when V_r = + 2.2 volt (charge time $\sim$1/2 hr.)

5. Photo, start discharge at $\sim$35 ma to determine D_1. (see note 2)

6. Photo, terminate discharge when V_r = +1.1 volt (discharge time < 1 hr.)

7. - 10. Same as Steps A.7 - A.10.

11. Photo, start discharge at 35 ma (see note 3)

12. Photo, terminate discharge when V_r = +1.1 volt (discharge time < 1 hr.)

13. Photo, generate end-of-test signal.

14. Calibration sequence.

15. Disconnect silver test cell.

16. Generate end-of-Task 2 signal.

17. Turn off circulating pumps.

TABLE 3-2

TASK 2 MEASUREMENTS

Measurands	Recorder Channel	Measurand Range	Resolution	Accuracy	Voltage Signal Available Volts (max)	Minimum Input Impedance	Sampling Rate Meas'ts/Min.	Test Time per Sample
A. Zinc Test Cell:								
Voltage: Zn electrode to ref.	1	-0.25 to +0.5V	10 MV	±30MV	+0.5	10K	Continuous	2.5 hours
Voltage: Cell	2	1.0 - 2.2V	20 MV	±50MV	2.2V	10K		
Cell Current (ma)	3	0 - 50	1 MA	±2.5MA	.065	10K		
Temperature(note 4)	4	0 - 50°C	0.1°C	1°C	.065	10K		
Elapsed Time	5	0 - 2.5 hrs.	1 sec.	10 sec.	←ref.freq.of→ tape recorder			
B. Silver Test Cell:								
Voltage: AG electrode to ref.	1	1.0 - 2.2	20 MV	±50 MV	2.2V	10K		
Voltage: Cell	2	1.0 - 2.2	20 MV	±50 MV	2.2V	10K		
Cell Current (ma)	3	0 - 50	1 MA	±2.5MA	.065	10K		
Temperature	4	0 - 50°C	0.1°C	1°C	.065	10K		
Elapsed Time	5	0 - 2.5 hrs.	1 sec.	10 sec.	←ref.freq.of→ tape recorder			

NOTES:

1. Initial charge current to be adjustable over range of 5-20ma.
2. D_1 is discharge capacity obtained under gas loaded conditions. Adjustment range on discharge current to be 10-50ma.
3. D_2 is additional discharge capacity gained by degassing electrode. Adjustment range on discharge current to be 10-50ma.
4. Ambient temperature near two test cells.
5. Cell electrodes are fixed in the horizontal position. The Task 2 control system provides a timed override which generates an end-of-test signal after 3 hours which will initiate the next test sequence.
6. V_r is voltage between test electrode and Zn reference electrode.

3.3 Description of the Test Equipment

Figure 3-1 shows a schematic diagram of the equipment arrangement for one of the cells in the Task 2 experiment. A sealless centrifugal pump is used to circulate the electrolyte past the test electrode of the cell, then through a 200 mesh nylon screen which acts as a gas separator, and back to the pump. The recirculating flow can be measured on a flowmeter installed in this circuit and regulated by means of a metering valve V4 which is an integral part of the flowmeter. The gas reservoir shown at the top of the cell is intended to provide expansion volume when gas is removed from the cell by reducing system pressure. A vent trap is provided between the vacuum source and the gas reservoir to handle any liquid which might be carried over during the evacuation process. This vent trap consists of nylon mesh screen contained in a teflon cylinder. A 3-way solenoid valve (SV1) permits evacuation of the cell when energized. In the de-energized position it vents the cell to ambient. The vacuum level reached in the system is controlled by manipulating two bleed valves BV1 and BV2 and observing the manifold vacuum on a panel mounted vacuum gage.

Prior to the test toggle valve V1 is closed and both the test cell and the KOH reservoir are evacuated. In the case of the latter this is done by opening electrolyte fill valve V3 to a vacuum source, and in the case of the former by energizing solenoid valve SV1. After evacuation and leak testing, the electrolyte reservoir is backfilled with a solution of 40% by weight KOH which has been thoroughly degassed prior to filling. After filling valve V3 is closed. Valve V2 provides a means for controlling flow rate as electrolyte is introduced into the system. To fill the cell, toggle valve V1 is opened while the cell is still connected to vacuum. The electrolyte is allowed to

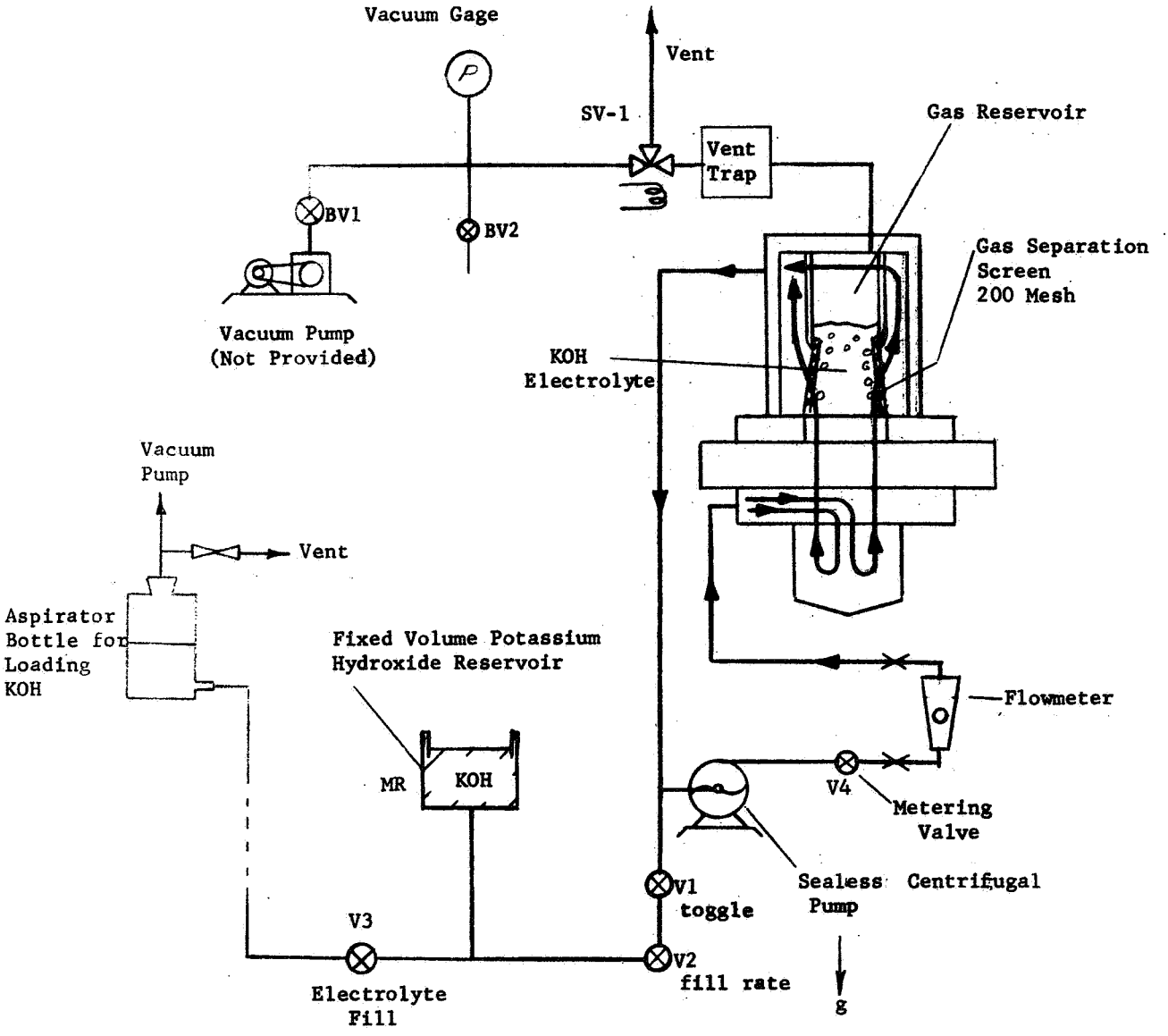

Figure 3-1. Schematic Diagram-Task 2 Experiment

gradually fill the system to any desired volume which can be visually monitored. When an adequate amount of electrolyte has been admitted, toggle valve V1 is closed.

An alternative approach which has been provided for is automatic filling with a fixed volume of electrolyte. This is accomplished by utilizing built-in stops on the electrolyte reservoir which can be set to admit any fixed volume of electrolyte to the system.

Once filling has been completed, solenoid valve SV1 is opened venting the system to ambient, and the centrifugal pump is turned on to provide circulation of the electrolyte. A similar cell and equipment arrangement is provided for testing both a zinc electrode and a silver electrode. The systems are completely independent except for the motor which drives the circulating pumps and the camera used to record bubble behavior. Figure 3.2 shows a photograph of the equipment arrangement on the front panel of the Task 2 panel. Two test cells are shown, one in which the zinc electrode, and the other in which the silver electrode, can be observed and photographed. The physical arrangement of the cells relative to the camera and lens assembly permits either of the test electrodes to be photographed. (Which electrode is photographed depends on which of the two flash units are activated.) This is accomplished by means of a special lens arrangement attached to the camera which provides for a simultaneous viewing of both test electrodes. The camera used is motor driven and provides for up to 36-35 mm photographs of test electrodes. The two flash units employed are operated from rechargeable batteries. They are positioned on either side of the lens assembly to provide illumination of one or the other test electrodes. Each of these units has a capacity in excess of the 10 photographs that are normally taken in testing any one electrode.

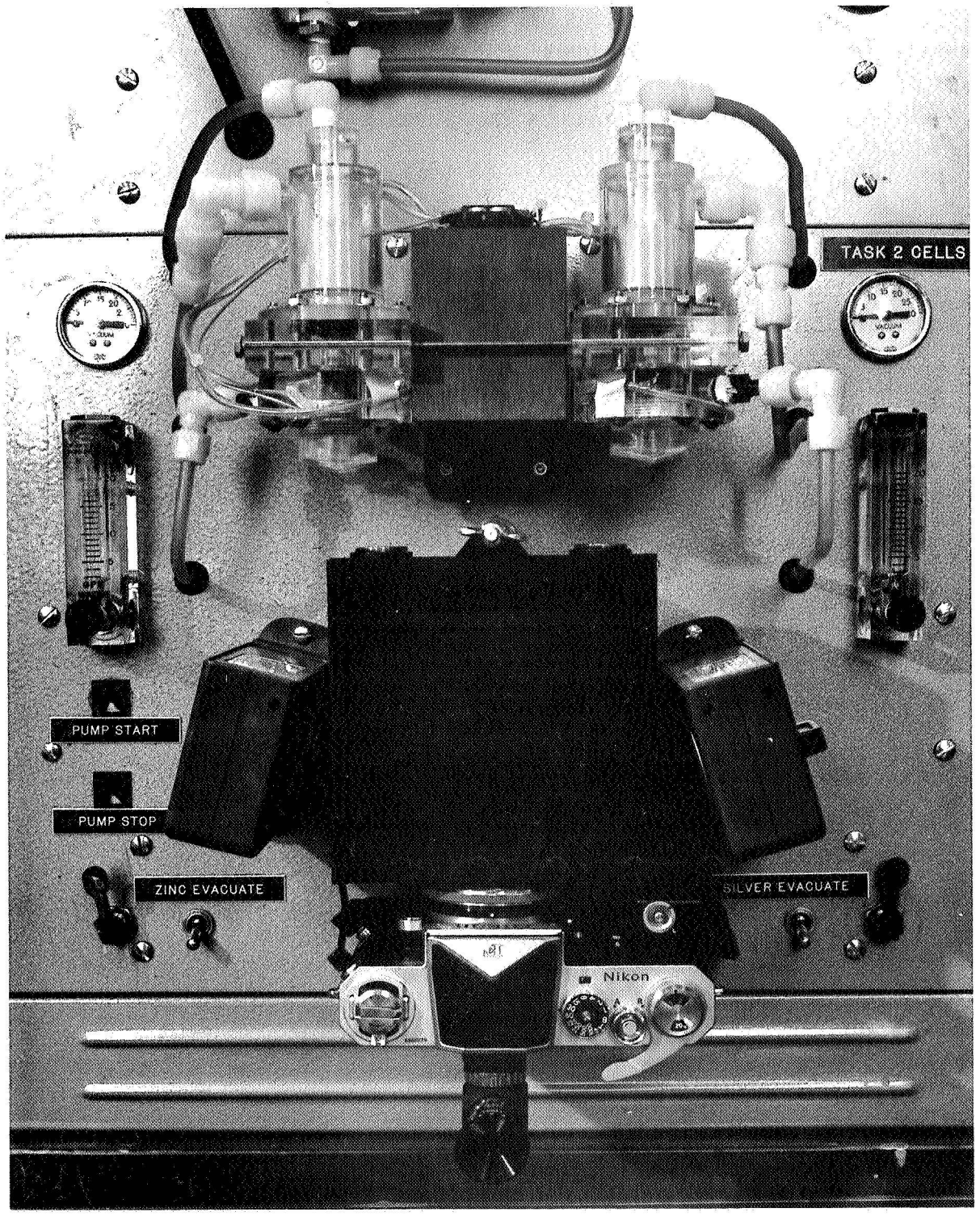

Figure 3.2. Task 2 Test Panel

On the rear of this panel and in the chassis associated with it are located the remainder of the fluid and gas handling components in this system. This equipment arrangement is shown in Figure 3.3. In the right and left foreground are the electrolyte reservoirs which are made of acrylic plastic, center foreground are the vacuum regulating manifolds for the two cells; behind these manifolds is the motor which drives two centrifugal pumps in the electrolyte recirculating systems, and located directly above a circuit board are the two vent traps. Except for some relays which control the camera and flash units and cell switching, which are located on the circuit board at the back of the Task 2 panel, all of the electronic controls and circuits are located in the main frame of the equipment.

An exploded view of one of the Task 2 cell assemblies is shown in Figure 3.4. The section to the left comprises the gas reservoir and gas separator. The rectangular block next to this is the main mounting block for the cell; to the right of this is the test cell itself, and to its right the viewing window for the test electrode. Each cell is provided with a zinc reference electrode. The gas separator and test cell are joined to the main cell mount through O-ring seals. Also, the viewing window is sealed to the cell body with another O-ring seal. This O-ring appears in Figure 3.5 which is a frontal view of the test cell body. In this photograph can be seen the front surface of the nickel wire grid covering the test electrode. The reference electrode is just above it and to the left of the orifice through which the electrolyte is circulated across the face of the electrode. To the right of this photograph a separate test electrode is shown prior to installation.

3.4 Activation and Test Procedure Changes

The activation procedure used is as shown in Section I of Table 3.1

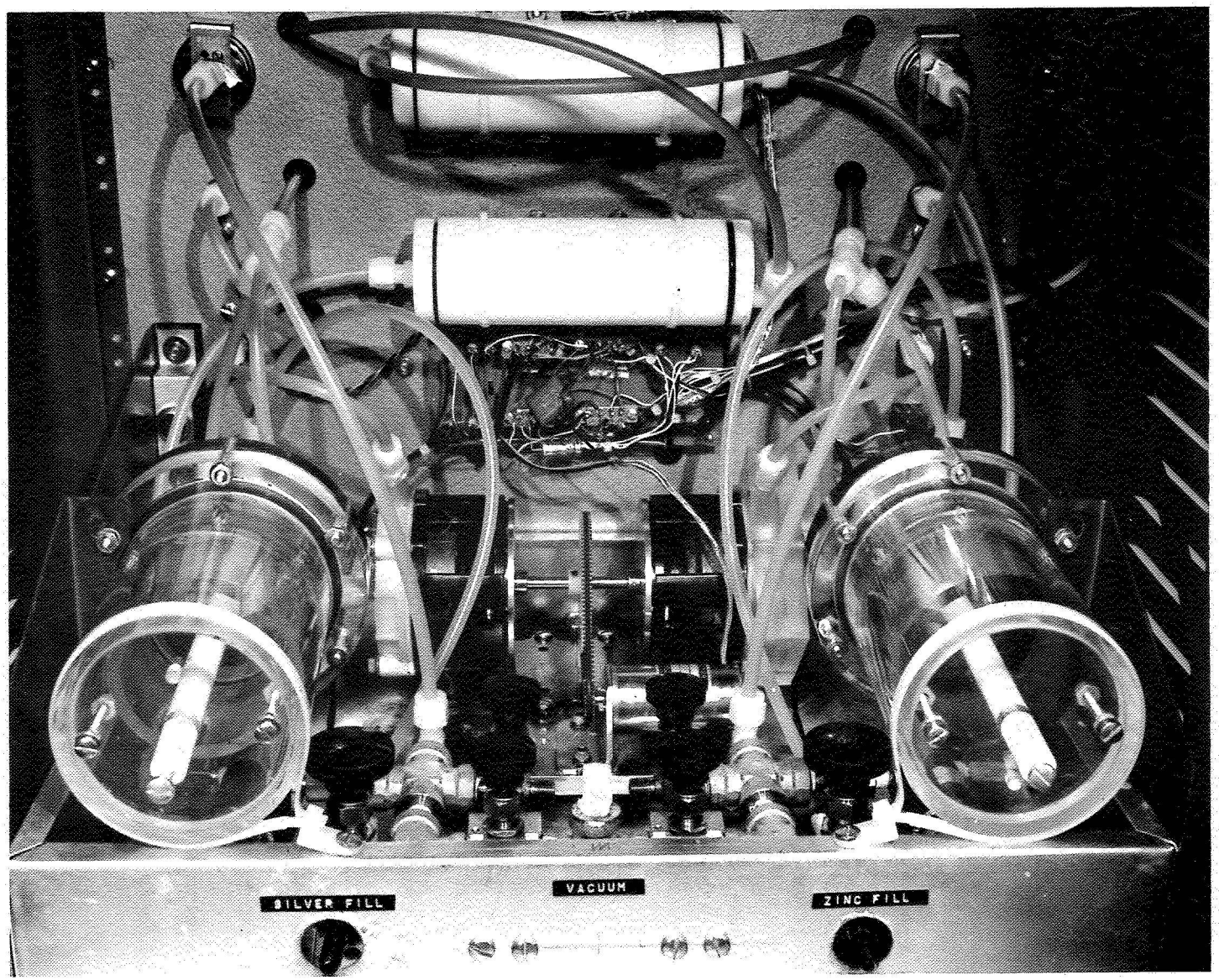

Figure 3.3. Task 2 Chassis With Electrolyte Reservoirs, Pumps, and Vent Traps

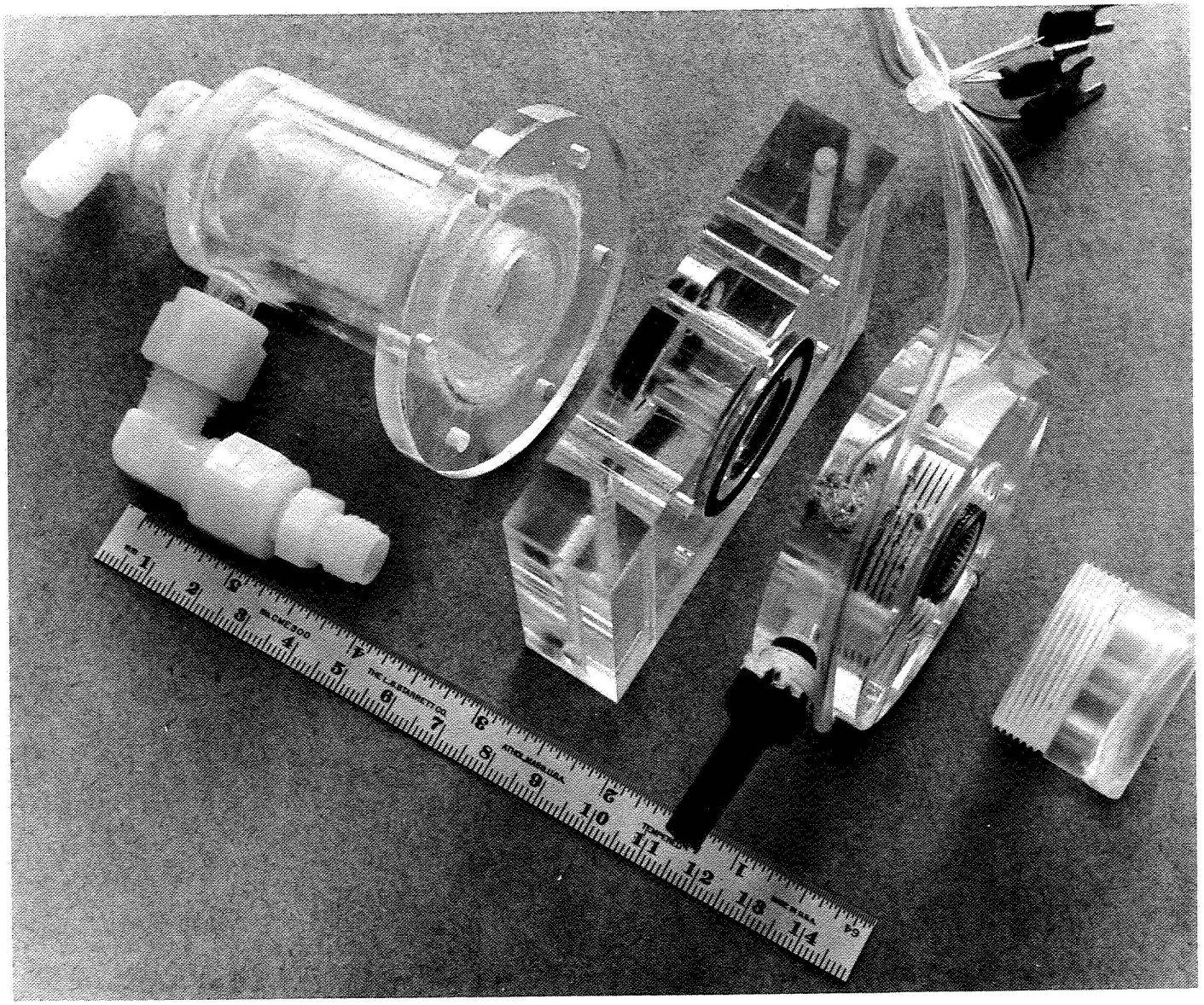

Figure 3.4. Exploded View--Task 2 Cell

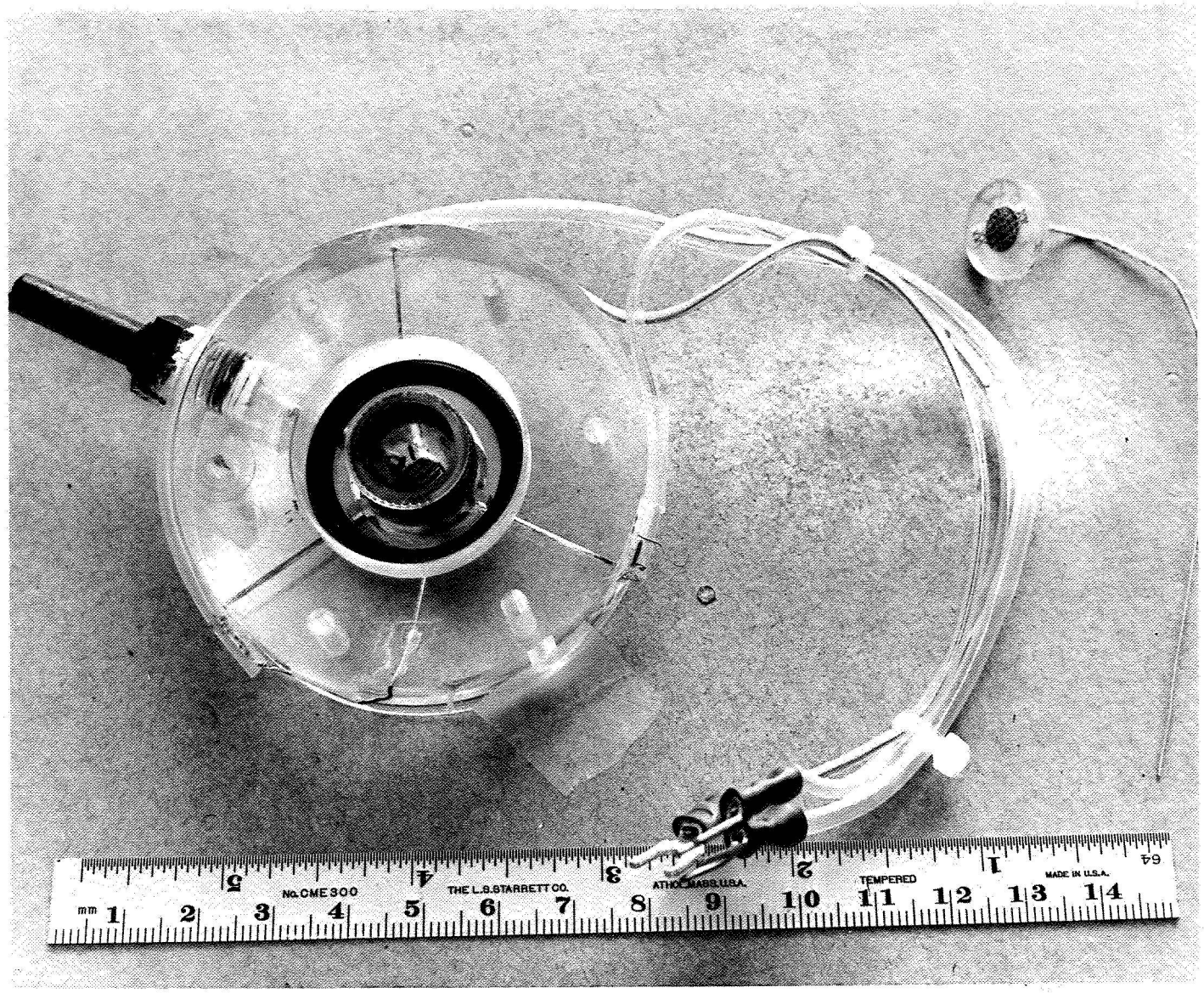

Figure 3.5. Task 2 Electrode Assembly, Bottom View

with one exception. Step 2 is now carried out after completing the venting of the system accomplished in Step 7. This change was made because it was found that the circulating pumps cavitated if they were allowed to operate during the filling procedure under vacuum. Therefore, they are not turned on until filling and venting is completed. Once turned on they remain in operation throughout the Task 2 automatic test sequence except when the cells are being evacuated. At that time, they are again turned off until the system pressure is returned to one atmosphere. The programming of the pump operation is carried out automatically by the Control Logic.

A number of minor revisions have been made in the automatic test sequence which was listed in Part II of Table 3-1. These are as follows:

(1) Photograph number 1 is taken at the beginning of Step 2.

(2) Following connection of the cell under test there is a one minute time delay before the test proceeds.

(3) Following the completion of Step 4 there is a two minute time delay before the discharge called for in Step 5 is begun.

(4) No photograph is taken in Step 6.

(5) During Steps 7 and 9 the recirculating pump is turned off.

(6) In Step 12 there is again a two minute time delay following completion of Step 12.

(7) The photograph at the start of Step 13 has been eliminated.

With these changes, a total of 10 photographs are taken during the course of any one cell test.

3.5 Test Records

A real time chart record of an automated test of the zinc test electrode is shown in Figure 3.6. The five channels of data recorded as indicated on

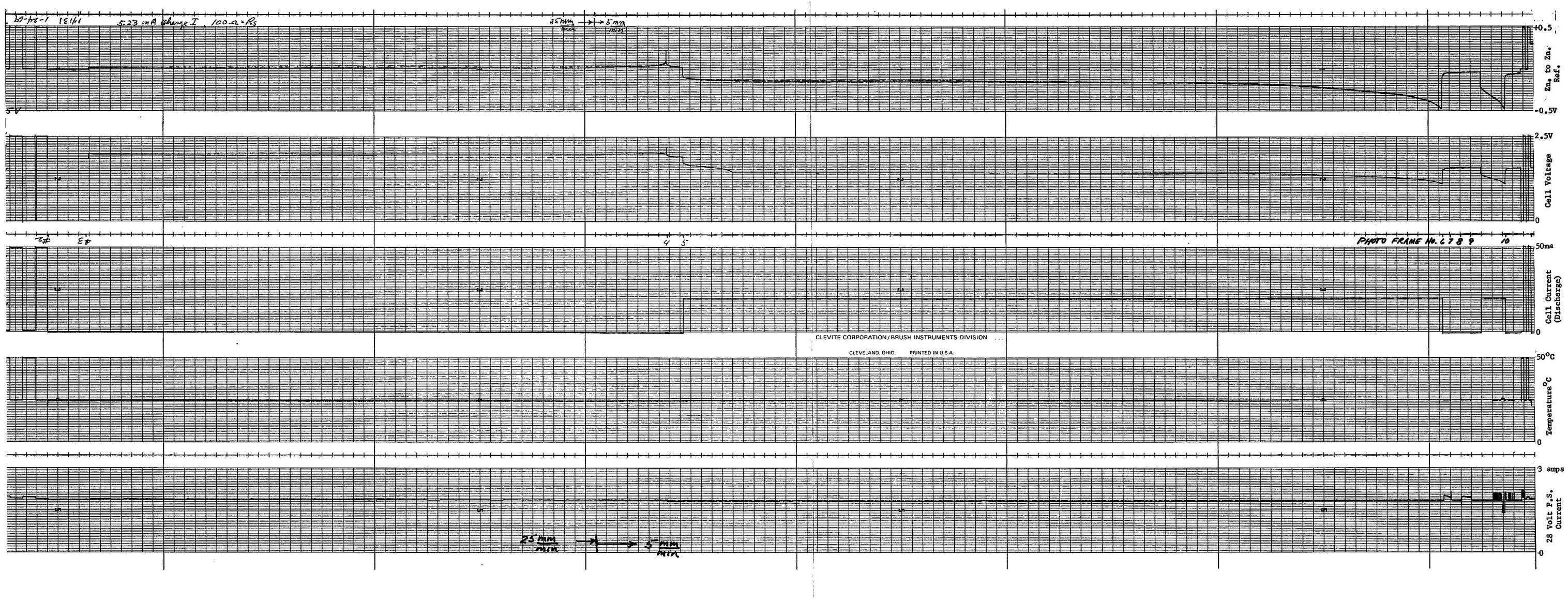

Figure 3. 6. Chart Record, Task 2 Experiment, Zn Test Electrode

the chart are:

(1) Zinc to Zinc reference potential.

(2) Cell voltage.

(3) Cell discharge current.

(4) Ambient temperature.

(5) Current drawn from the 28 volt supply.

Between the second and third channels, a marker pen is used to indicate when a photograph is taken, and the numbers associated with these marks are the photograph numbers for this test series. Four of the photographs taken during this test are shown in Figures 3.7 and 3.8.

The first figure contains photograph numbers two and four of the test sequence. The first of these was taken at the start of the test before the cell was charged, while the second was taken at the end of the charge cycle.

In these photos, the light areas are an indication of gas loading between electrode and cellophane, or alternatively, they may be due to reflected light from metallic zinc particles on the electrode surface or some combination of the two effects. The latter seems to best fit the photographic observations. For example in Figure 3.7, two photographs (#2 and #4 of the test sequence) show the zinc electrode at the start of test before charging, and at the end of the charge cycle. There is little change in appearance which suggests a negligible gas build up and probably the light areas present are caused by zinc crystals. In Figure 3.8 the two photographs were taken at the end of the first discharge cycle, and at the end of the second discharge cycle. Comparing the first of these to Figure 3.7 shows a considerable decrease in light reflecting areas, which is consistent with a conversion of zinc to zinc oxide on discharge. Reduction of gas loading would not be

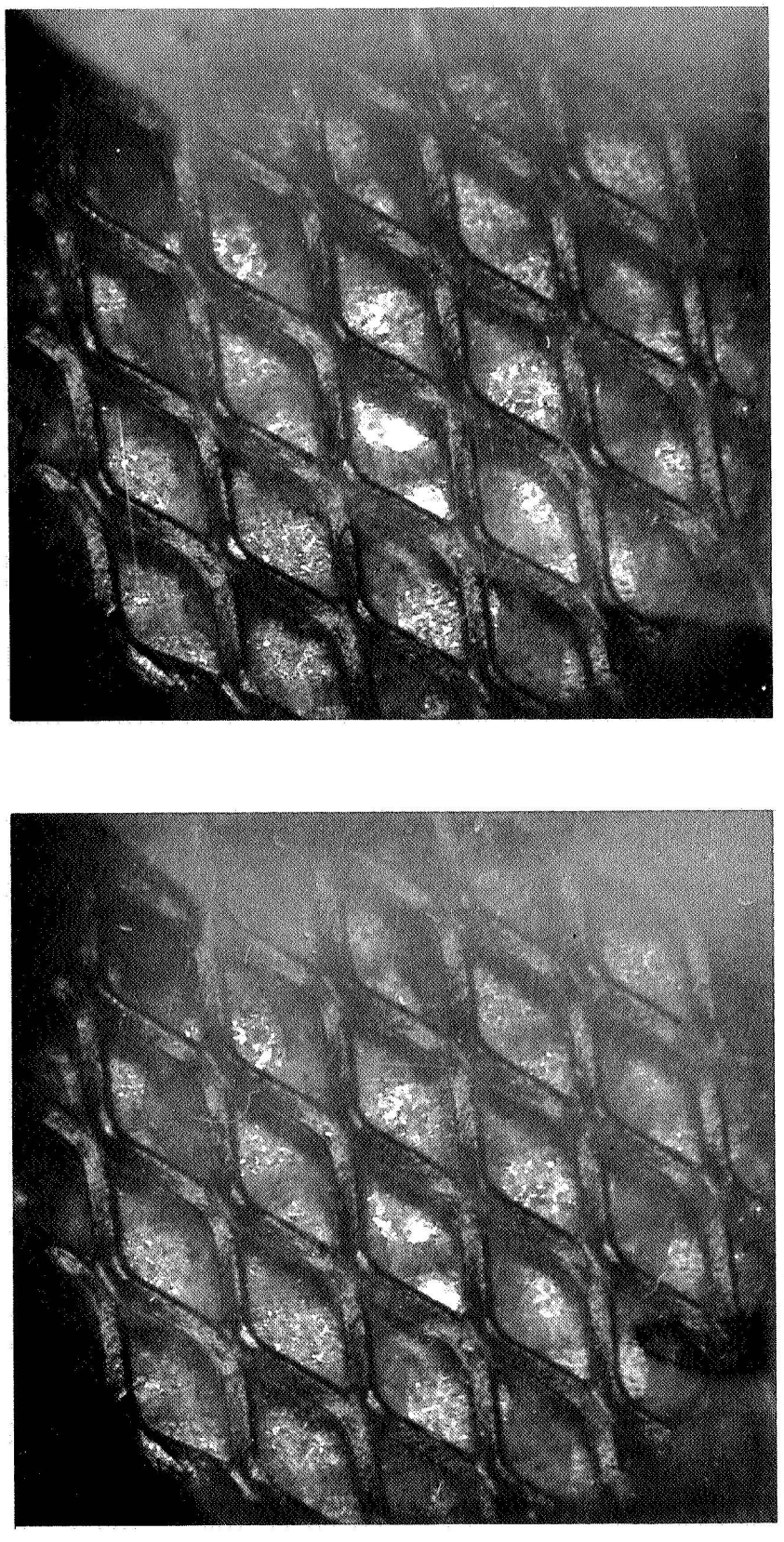

Figure 3. 7. Photographs of Zn Test Electrode
Upper: Start of Test
Lower: End of Charge

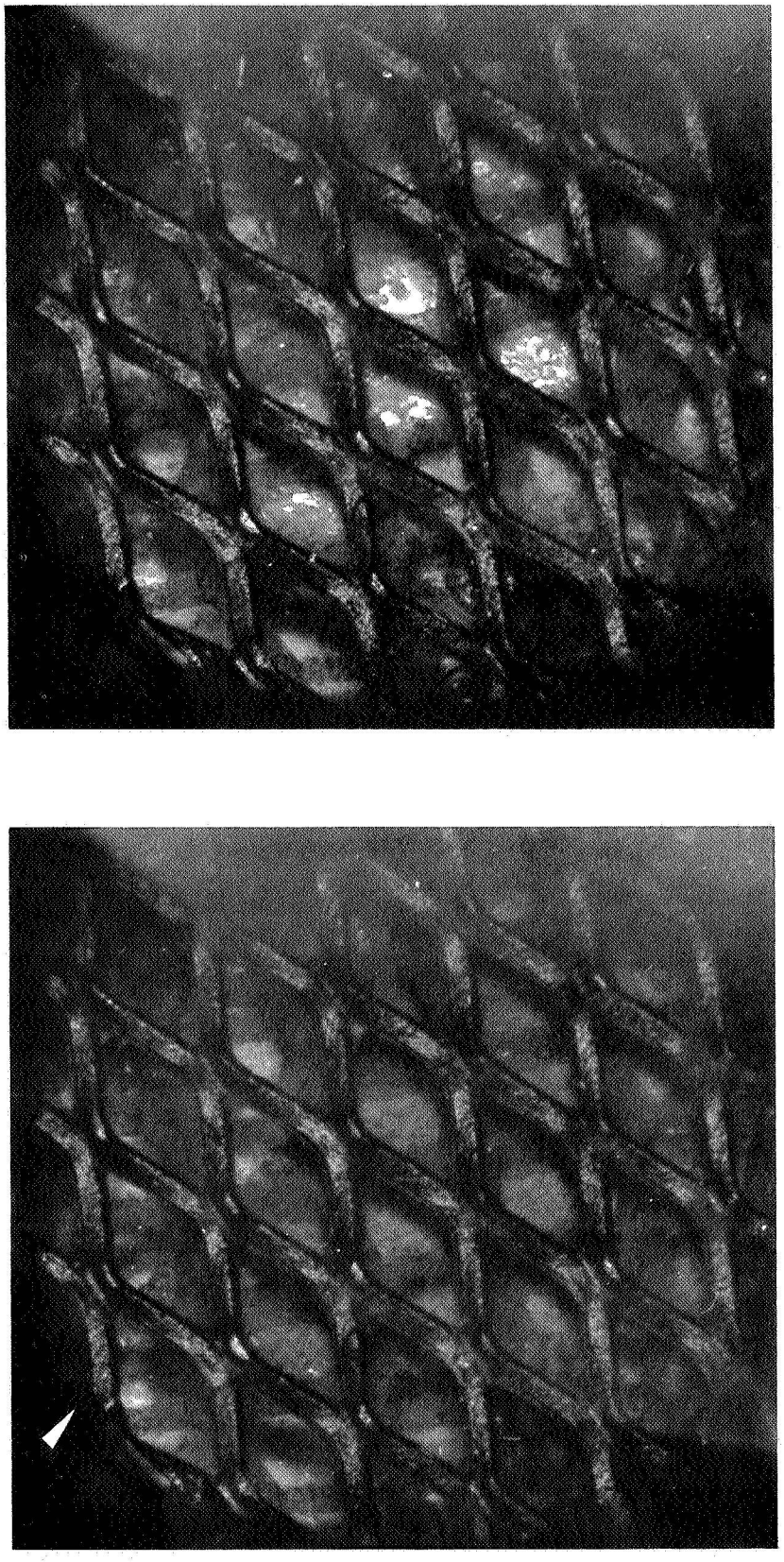

Figure 3.8. Photographs of Zn Test Electrode
Upper: End of First Discharge
Lower: End of Second Discharge

expected on discharge. Those larger light reflecting areas remaining are probably gas coverage which is rather sparse. This is consistent with the results of the second photo of Figure 3.8 which shows these reflecting areas are missing after the evacuation and backfill cycles, indicating removal of what gas coverage was present. Intermediate photographs in this series showed that the majority of gas was removed in the first evacuation-backfill cycle, while the small amount of gas remaining, was apparent during the second evacuation cycle, but disappeared on backfilling. The behavior of the light areas in the series of photographs is fairly conclusive evidence that they represent both light reflected from zinc and to some extent from gas bubbles behind the cellophane separator. Also evident, however, is the fact that under these test conditions there appeared to be little additional gas generation during the charge cycle. This, plus the fact that there was very little residual discharge capacity (e.g. D2/D1 was of the order of .03 instead of greater than 1.0 as in previous bench tests) indicates that the degree of gas loading of the electrode was probably insufficient to significantly affect the electrode discharge capacity.

A similar test was run on the silver electrode with similar results. Very little additional discharge capacity was found in the second discharge after evacuation and backfilling. In this case the photographs showed no perceptable change in the gas cover during the course of the test. The reason for this is a darkening of the cellophane separator believed to be due to a reaction with the silver ion from the electrode. This darkening apparently causes a highly reflective coating on the separator which prevents observation of bubble movements behind it. A sample photograph taken during the course of this test on silver is shown in Figure 3.9.

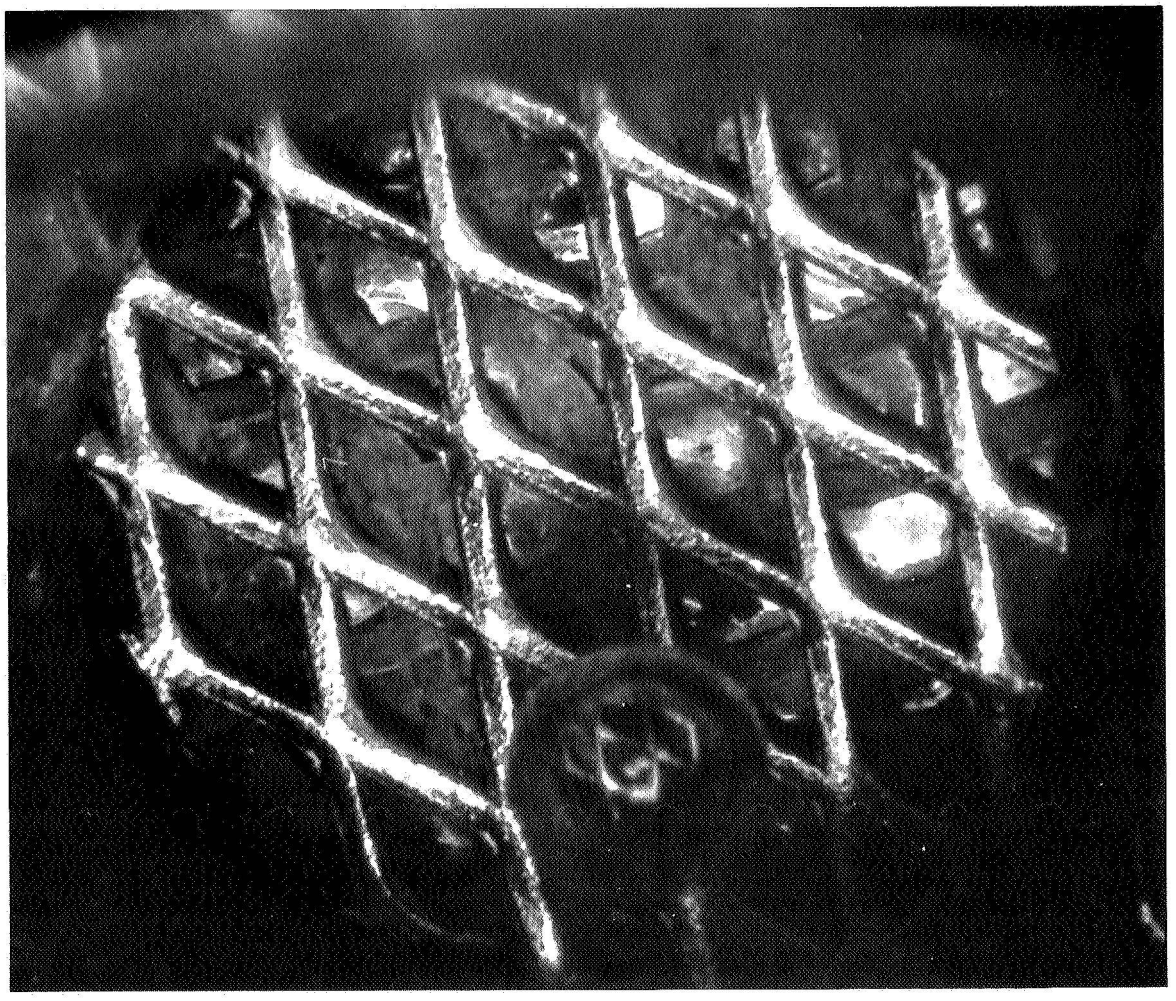

Figure 3. 9. Photograph of Silver Electrode, Task 2 Experiment

3.6 Test Results

While the tests conducted to date on the Task 2 equipment have shown adequate performance on the part of the test control equipment, it has not been possible to date to record test electrode performance as was noted in the previous bench top tests which were manually conducted.

There are a number of possible explanations for this discrepancy. One is that the initial charge of the cell was not carried out in a way which would permit adequate gas coverage of the electrode surface. If this were the case, results similar to those obtained on the zinc test electrode would be expected. Another is that differences in the construction of electrodes inhibited gas blockage e.g. due to close contact between cellophane and electrode surface. In an effort to investigate the former possibility some additional tests have been run where test parameters were varied in an effort to emphasize gassing and insure a greater degree of electrode coverage.

In one test on the silver electrode, the charge current was reduced from the normal value of 12 milliamps to 4 milliamps to provide a longer charge time and facilitate a larger gas buildup. At this lower charge rate the charge time was very long and the cell voltage did not rise to terminate the charge cycle; consequently after about two hours, the charge current was raised to terminate the charge cycle. During this period there was considerable gas evolution observed from the cell electrodes. At the first evacuation cycle there was evidence of a significant volume of gas trapped in the centrifugal pump. The effect of expansion of this gas was to drive electrolyte from the cell into the vent trap. In order to prevent this it was necessary to reduce the vacuum level to 25 In. Hg. to prevent liquid carryover. Under these conditions, the second discharge showed a negligible increase in capacity which is not surprising in view of the inefficiency of gas removal at this

vacuum level.

While this particular test represented an extreme in terms of the amount of gas generated, it and other similar tests indicate that the gas-liquid separating system built into the cell is probably not efficient enough to handle those conditions where adequate gas generation occurs in an electrode. While the amount of gas circulating in the system is not objectionable from the standpoint of the photography, its accumulation in the pump is. Since the centrifugal pump when operating, is a more efficient gas separator then the nylon screen section in the cell, over a period of time the pump accumulates a gas pocket which cannot be effectively removed during the subsequent evacuation cycle.

The possibility of preventing this by operating the circulating pump infrequently has been considered but this does not appear to be a workable solution. Without the circulating pump functioning, gas build up very quickly occurs across the face of the test electrode and quickly reduces the charge rate to extremely low levels. The circulation afforded by the pump is necessary to insure an adequate charge current under gassing conditions.

In the case of the silver electrode a special problem has arisen due to the darkening of the cellophane separator even after relatively short exposure to electrolyte. This darkening quickly eliminates the possibility of photographing gas bubbles behind the separator, since the separator itself becomes a very highly reflective surface. This may necessitate finding a different separator material for use with the silver test electrode.

3.7 Discussion of Test Results

In view of the surprisingly low D_2/D_1 ratios obtained during our most recent test runs at high discharge current densities, it may be useful to review in greater detail the basic features and consequences of localized gas trapping, discussed earlier[2] and illustrated in Figure 3.10. In these cross-sectional, highly magnified views of various hypothetical test electrodes of the type used in this Task 2 program, only the most salient features are shown, namely the fablok weave, holding the membrane spearator against the porous test electrode. Not shown is the electrolyte, which penetrates all parts and the expanded nickel screen which provides the compressive force.

Figure 3.10A illustrates the "ideal" electrode with uniform and perfect contact between the membrane separator and the test electrode. Any trapped gas generated during charge or open circuit condition conforms to the porosity of the test electrode, leaving a large number of pathways for the ionic discharge current to reach all volume elements of the test electrode. The D_2/D_1-ratio to be expected for such an ideal electrode is, of course, very small. The small trapped gas bubbles of Figure 3.7A do <u>not</u> contribute to the specular reflection of light, for which this particular cell configuration is optimized. In fact, they may be very hard to see or photograph at all.

In Figure 3.10B <u>small</u> regions of specular reflection begin to appear because the trapped gas bubbles are much larger now. The localized separation shown between the membrane separator and the test electrode can be caused, for example, by excessive swelling of the membrane. Even here the D_2/D_1-

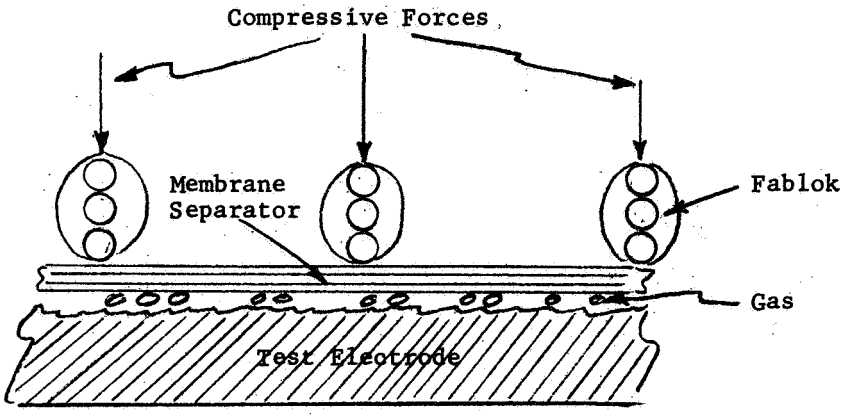

$$\frac{D_2}{D_1} \ll 1$$

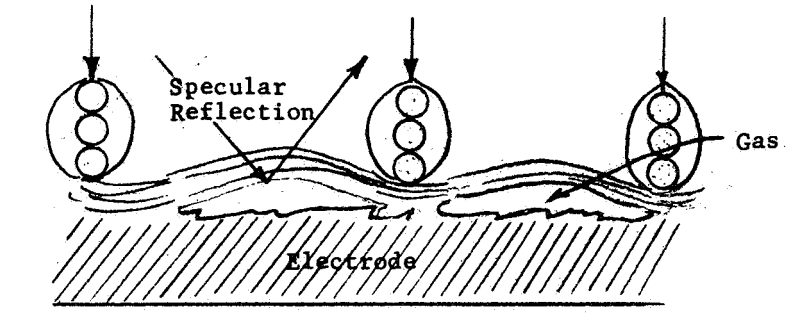

$$\frac{D_2}{D_1} \approx 0.5\text{-}1$$

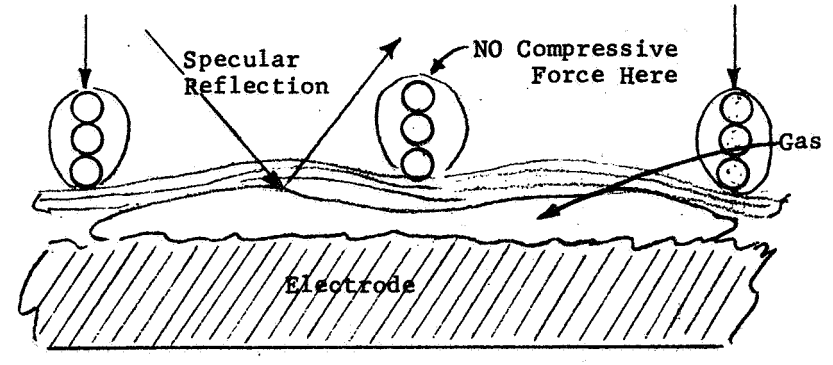

$$\frac{D_2}{D_1} > 1$$

Figure 3.10. Cross-Sectional View of Various Test Electrodes

ratios to be expected are as yet not very large because the blocking action of the trapped gas does not extend over regions large compared to the thickness of the test electrode.

Adding to this now, the absence of localized compressive forces on the fablok as illustrated in Figure 3.10C, individual trapped gas bubbles may extend over regions large compared to the thickness of the test electrode. Under these conditions gas passivation becomes very severe, as indicated by the large D_2/D_1-ratios to be expected. Conditions A, B, and C can conceivably occur side by side on the same test electrode. In all probability they are applicable also to commercial electrode configurations.

Our latest test results, giving low D_2/D_1-yields and little or no specular reflection, seem to indicate the prevalence of the "ideal" electrode structure (3.10A). Earlier results are clearly more in line with configurations 3.10B and 3.10C.

One of the fringe benefits of the present Task 2 study may be the development of a new method for the detection and measurement of gas trapping in commercial electrode systems. The determination of D_2/D_1-ratios in conjunction with evacuation steps as described, measured as a function of orientation and/or gravity, may yield valuable information on the performance of commercial batteries under different operating conditions.

3.8 Discussion of Equipment Revisions

From the results discussed above it is concluded that some revisions must be made either in the test sequence or the test equipment in order to provide a workable Task 2 experiment. On the one hand it appears that test revisions will be necessary to insure a greater degree of gas formation at

the electrode surface, and possibly the use of greater discharge current densities in order to accentuate the effect of this gas coverage. Such changes can be made quite readily with adjustments built into the test equipment. If the use of a longer charge time is found to be an effective solution to the lack of gas coverage it should be possible to change the three hour time limit with minor modifications to the equipment.

It appears that the major problem involved in using such a modified test program is the inadequacy of the gas management system. This is not so much due to inefficiency of the separator built into the Task 2 cell, as the fact that the centrifugal pump when operating is a very effective gas separator in itself. Unfortunately, gas trapped in the pump is practically impossible to remove. Its expansion during the evacuation cycle tends to force electrolyte from the system and this cannot be tolerated.

However, certain changes could be made which may help significantly. One could consider the elimination of the centrifugal pump and substitution of some other type of pump e.g. peristaltic action, which would not show the same tendency to gas trap. However, the original choice of pump type was made on the basis of circulation needs, weight, and power efficiency. A change to a different type of pumping system would probably be made at a cost in size, weight, and power consumption. Another possibility would be to change the Task 2 cell design to minimize gas trapping near the test electrode. With the present design, particularly when operated under 1 g conditions, the cone supporting the auxiliary electrode tends to trap out any bubbles emanating from the pump system. Eddies formed about the electrolyte jet tend to trap bubbles which then grow and eventually become large enough so that buoyancy effects carry them upward. Eventually they deposit on the

test electrode where they are trapped. A redesign of the support structure for the auxiliary electrode may greatly reduce this tendency of bubble trapping, and therefore permit the recirculating pump to be used less frequently. Another possibility would be a revision in the test electrode fabrication procedure to allow more space for gas distribution behind the separator. The fact that some of the electrode photographs show zinc particles indicates very close spacing and probably high contact pressure between the cellophane separator and electrode, which may be inhibiting gas expansion and distribution.

A fourth possibility which has considerable appeal, would involve a redesign of the cell housing to eliminate the nylon screen gas separator, and use instead the centrifugal recirculating pump as a separator. This would make use of the high efficiency of the pump as a gas separator, which in the current system is a serious detriment. With this approach, the re-circulating pump would probably be repositioned so that it was closely coupled to the cell. Then any gas evolved in the cell would be quickly drawn into the pump and trapped. Gas evacuation would then have to be carried out from the center of the impeller housing. This could probably be done with the pump running. The main requirement in making this type of system functional, would be to insure that no gas accumulation occurred in the rest of the system. Such gas would expand as pressure was reduced and cause problems similar to those encountered with the present arrangement. It seems likely, however, that with the high separation efficiency of the pump, and by maintaining good circulation through the cell, the residence time of any bubbles in the cell could be minimized and a gas buildup avoided. This approach would represent a substantial change in the design of cell and

gas separating system, but very little change would be necessary in the control logic for the experiment. A particular advantage of using the centrifugal pump would be its insensitivity to gravitational forces. The fact that it works effectively under one gravity would indicate that it should be even more effective under zero gravity conditions.

However, before such additional development work were undertaken, it would seem advisable to run this equipment as it stands and gain more experience on the precise conditions necessary to emphasize gas loading effects.

4.0 TASK 3 EXPERIMENT DESCRIPTION

The purpose of Task 3 is to investigate the degradation of commercial cells under stress. The tests involve an initial capacity and polarization measurement, a series of five stress cycles and a final polarization and capacity measurement. Cell degradation can be assessed by a comparison of the initial and final capacity and polarization measurements. The initial test conditions are as follows:

Polarization:	0 to 15 amp current ramp
Capacity Discharge:	C rate, 5 amps
Capacity Charge:	C/5 rate (average), 2.5 amps initial
Stress Discharge:	65% DOD (rated capacity)
Stress Charge:	C rate, 5 amps initial
Polarization Discharge:	65% DOD (rated)

Provisions are made for sequentially testing six cells with a calibrating sequence between each cell test.

4.1 Cell Activation and Test Sequence

The Yardney HR5-DC7A cells were activated according to the manufacturers directions and using the Yardney supplied KOH electrolyte. The cells were allowed to soak for a minimum of 72 hours before the tests were begun.

The test sequence for each cell is the same and is listed in Table 4-1, on the following page.

4.2 Equipment Description

The description of the Task 3 test equipment has been covered in the Quarterly Reports, Test Plan, and Instruction Manual and will not be repeated here. Only those items that have not been noted before or have been

TABLE 4-1

Test Sequence for Task 3 Cells

1. Stress Discharge
2. Capacity Charge
3. Capacity Discharge
4. Capacity Charge
5. Polarization Discharge
6. Polarization
7. Stress Charge
8. Stress Discharge
9. Stress Charge
10. Stress Discharge
11. Stress Charge
12. Stress Discharge
13. Stress Charge
14. Stress Discharge
15. Stress Charge
16. Stress Discharge
17. Capacity Charge
18. Polarization Discharge
19. Polarization
20. Capacity Charge
21. Capacity Discharge

significantly changed are covered.

The cells are mounted on the rear of the Task 3 Control chassis. A photograph of the cell arrangement is shown in Figure 4.1. A thermistor is attached to each cell beneath a piece of adhesive backed foam rubber. The thermistor is mounted on the right side of each cell and is located near the center of the electrode structure. The adhesive holds the thermistor in place and the foam rubber provides a certain amount of thermal insulation.

The Task 3 Control Chassis contains not only the Task 3 circuitry but also the circuits to accommodate several important functions. The Task 3 Control Chassis contains the relays that provide the calibrating voltages, measurand switching and power supply switching. In addition all of the relay driver circuits are located on this chassis on printed circuit boards. A photograph of the chassis layout is shown in Figure 4.2.

There are several controllable variables associated with the Task 3 test. These variables along with their ranges are listed below.

TABLE 4-2

Controllable Parameter Ranges - Task 3 Experiment

1.	Charge Level Sensor Voltage:	.54 to 10v
2.	Discharge Level Sensor Voltages:	.45 to 2.4v
3.	Polarization Level Sensor Voltage:	0 to 10v
4.	Cell Rejection Level Sensor Voltage:	0 to 10v
5.	Stress Discharge Current:	0.7 to 20 amps
6.	Polarization Discharge Current:	0.7 to 20 amps
7.	Capacity Discharge Current:	0.14 to 10 amps
8.	Polarization Ramp Current:	0 to 20 amps
9.	Polarization Ramp Rate:	1 sec. to 20 min./f.s. current
10.	Stress Charge:	0 to 10 amps
11.	Capacity Charge:	0 to 10 amps

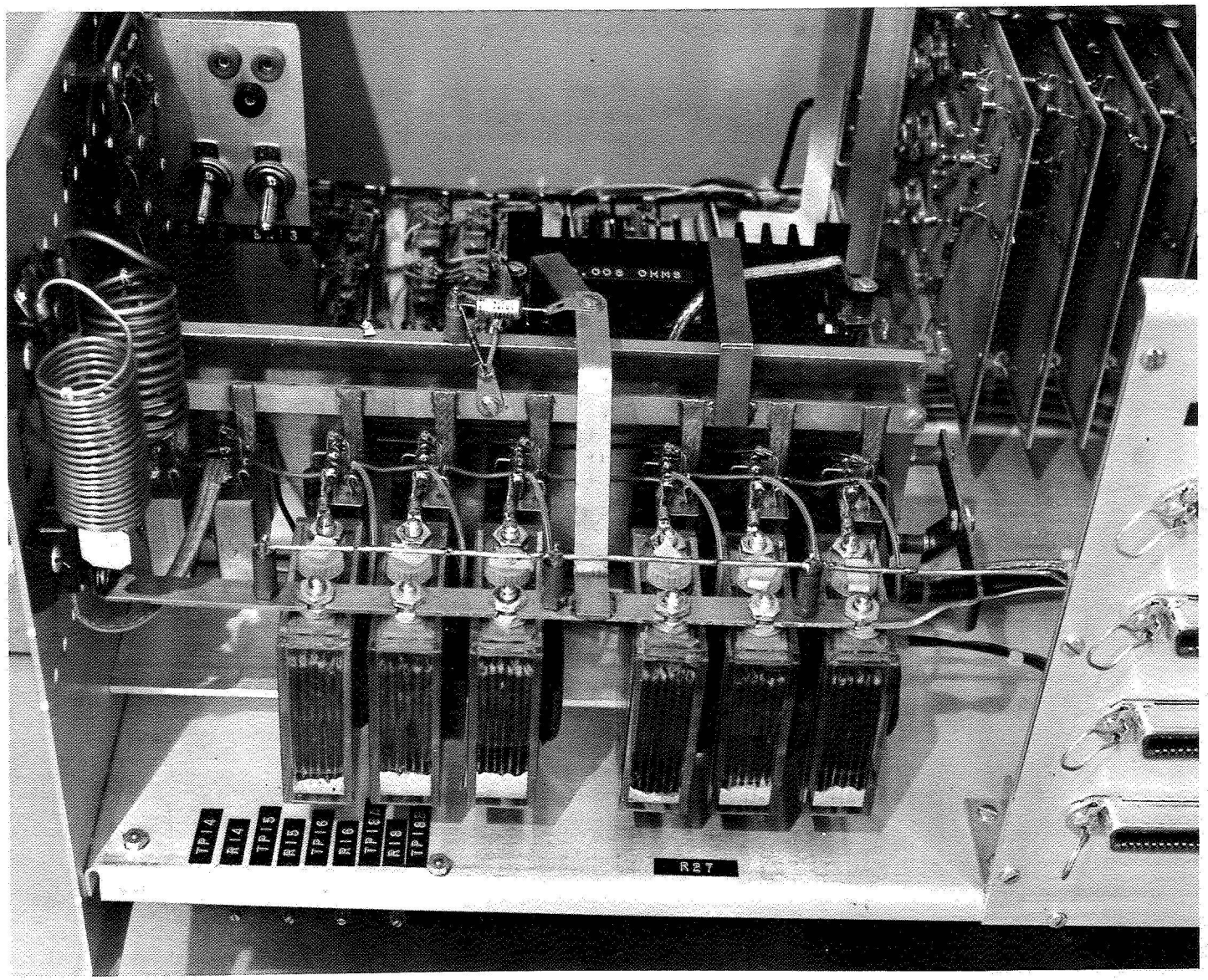

Figure 4.1. Task 3 Chassis, Cell Mounting Arrangement

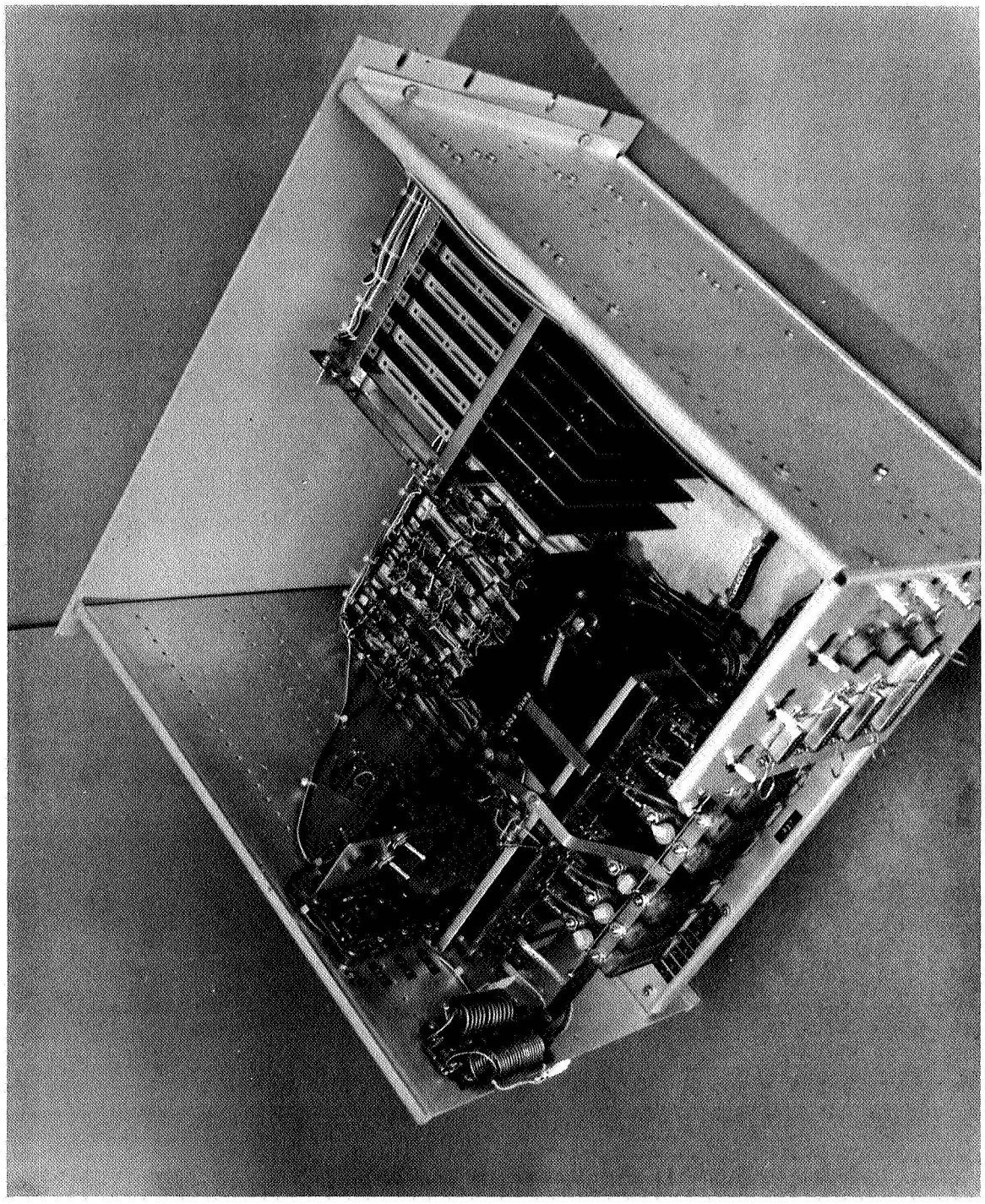

Figure 4. 2. Task 3 Chassis Layout

4.3 Test Records

There are four test records shown in the following figures. Figure 4-3 is the real time chart record of cell #15 which was tested at 65% DOD. Figure 4-4 is the real time record of cell #20 which was tested at 100% DOD. Figure 4-5 is the real time record of cell #20 which was tested for a second time at 100% DOD. Figure 4-6 is part of the playback record of cell #20 during its second test at 100% DOD.

The channel identification of the three real time records is as follows:

Channel 1 - Charging current, stress charge: 0 (center) to 18.5a
capacity charge: 0 (center) to 5.93a

Channel 2 - Cell Voltage, 0 to 2.5 volts

Channel 3 - Discharge Current, 0 to 15 amps

Channel 4 - Cell Temperature, 0 to 50^{o}C

Channel 5 - 28 Volt Power Supply Current, 0 to 3 amps

Channel 6 - 2.5 Volt Power Supply Current, 0 to 7.5 amps

The channel identification for Figure 4-6 is the same as above except that Channels 5 and 6 were not recorded on the tape and are therefore missing from the playback record.

The magnetic tape playback record was made on a Sangamo Electric tape recorder. The playback speed was 1 7/8 inches/second. The data recording during Task 3 is done in a sampled mode so that 14 seconds of data are recorded every 72 seconds. The tape is at rest in the machine during the remaining 58 second period. These periods of rest produce signals on the tape which appear to be noise to the F.M. electronics of the playback

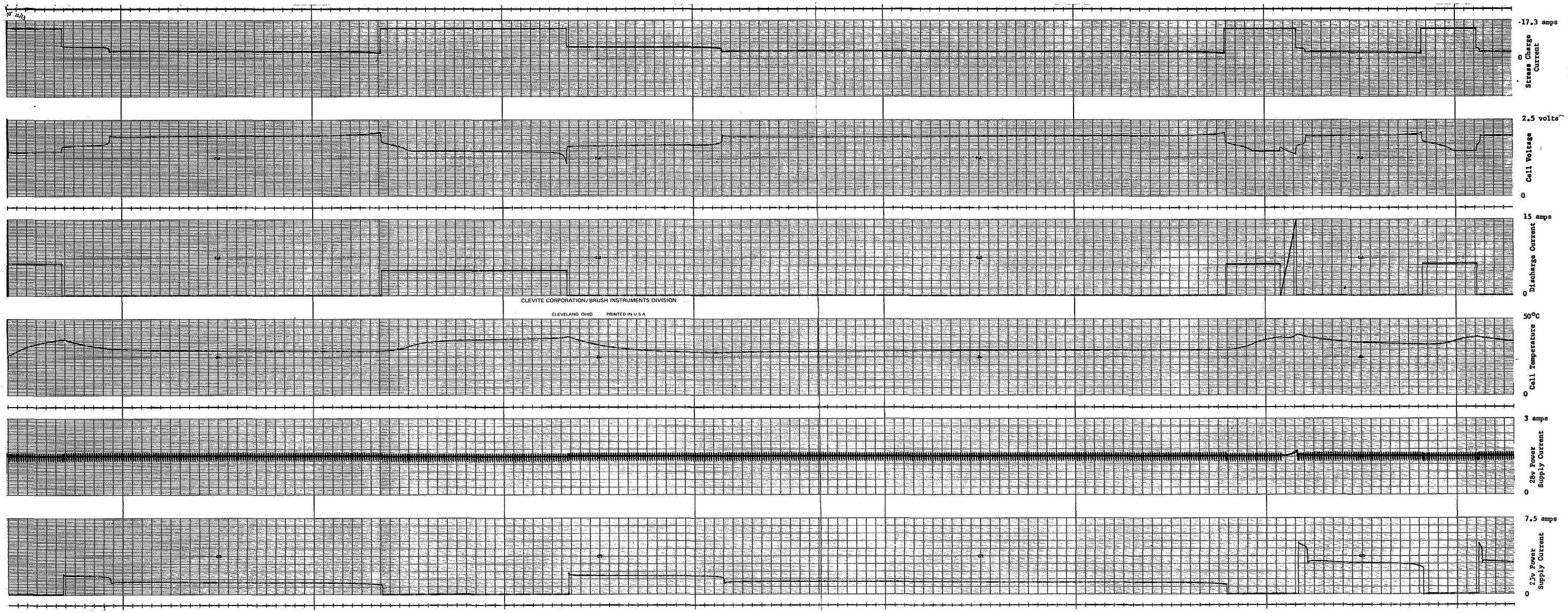

Figure 4. 3a. First Section, Task 3 Test Record, Cell #15, Tested at 65% DOD

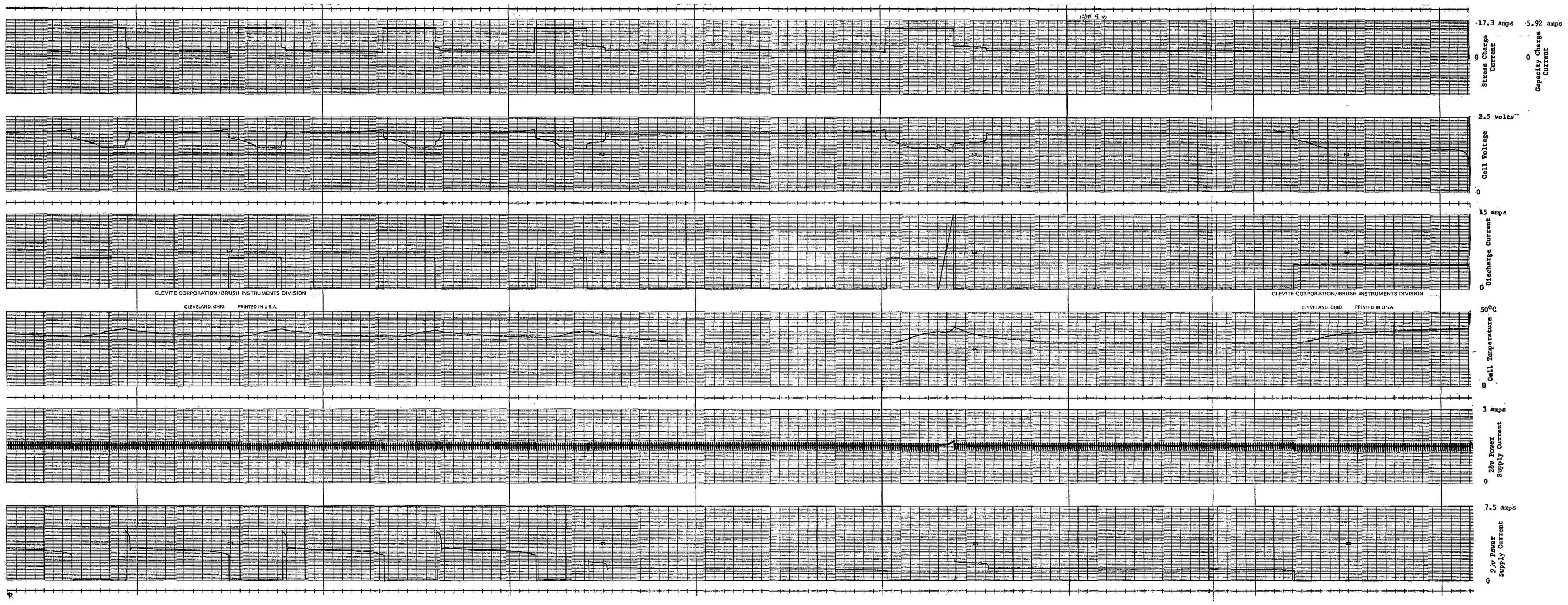

Figure 4. 3b. Second Section Task 3 Test Record, Cell #15, Tested at 65% DOD

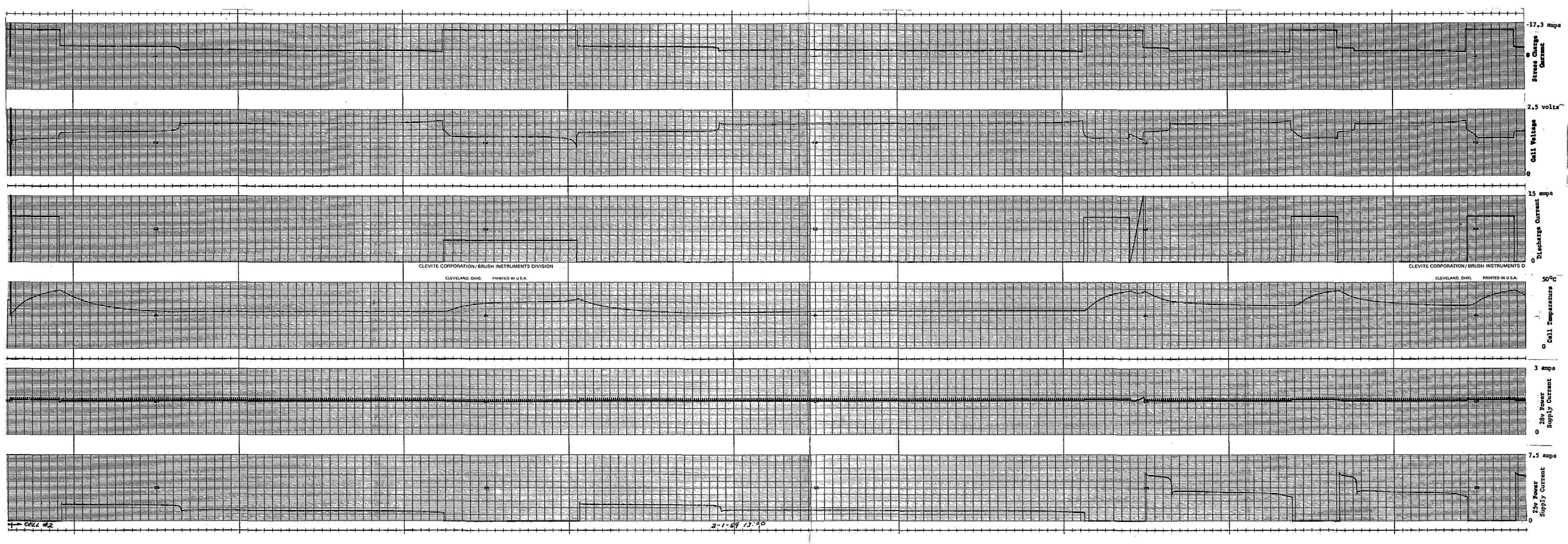

Figure 4.4a. First Section, Task 3 Test Record, Cell #2 Tested at 100% DOD

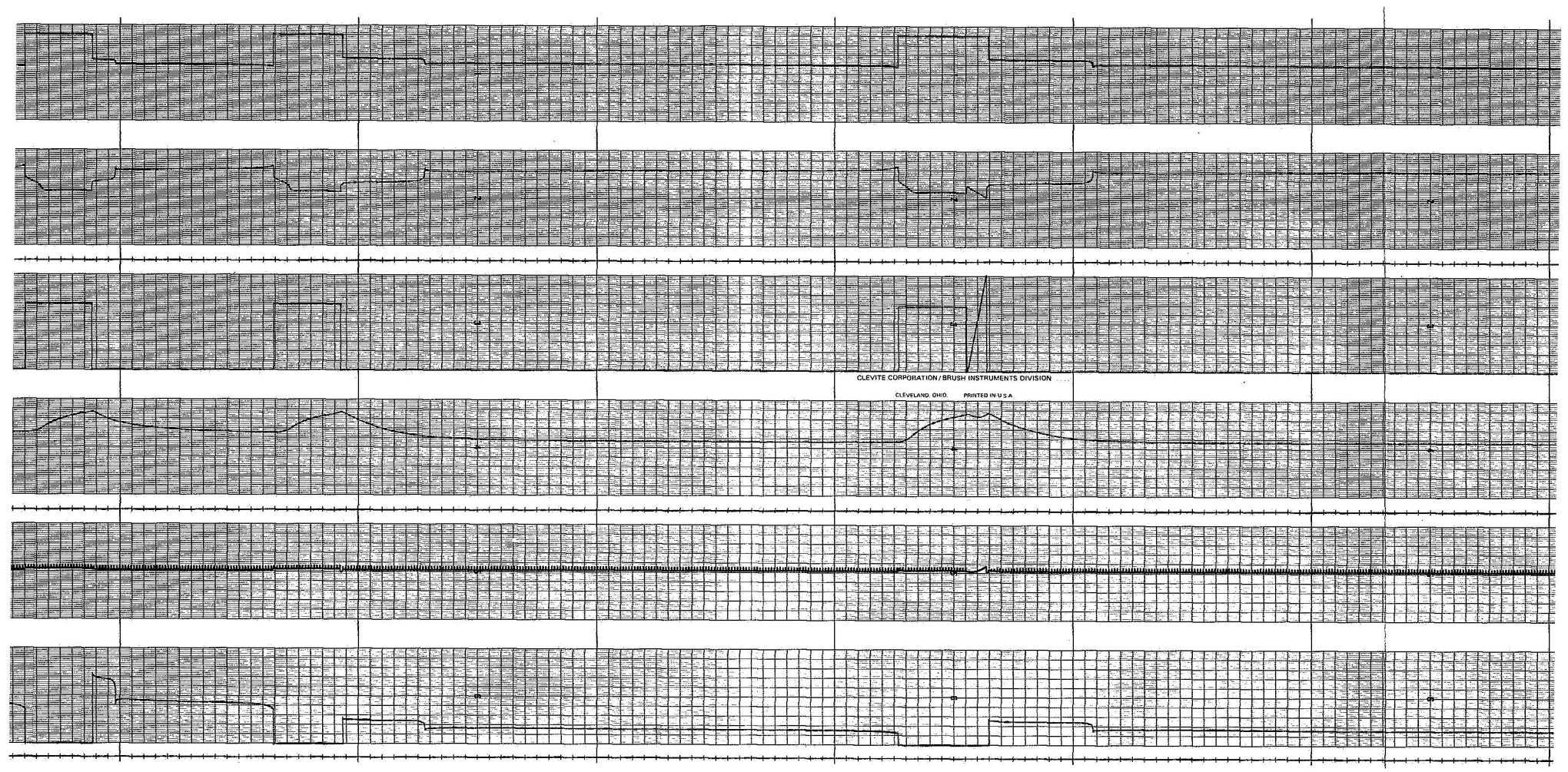

Figure 4.4b. Second Section, Task 3 Test Record, Cell #20, Tested at 100% DOD

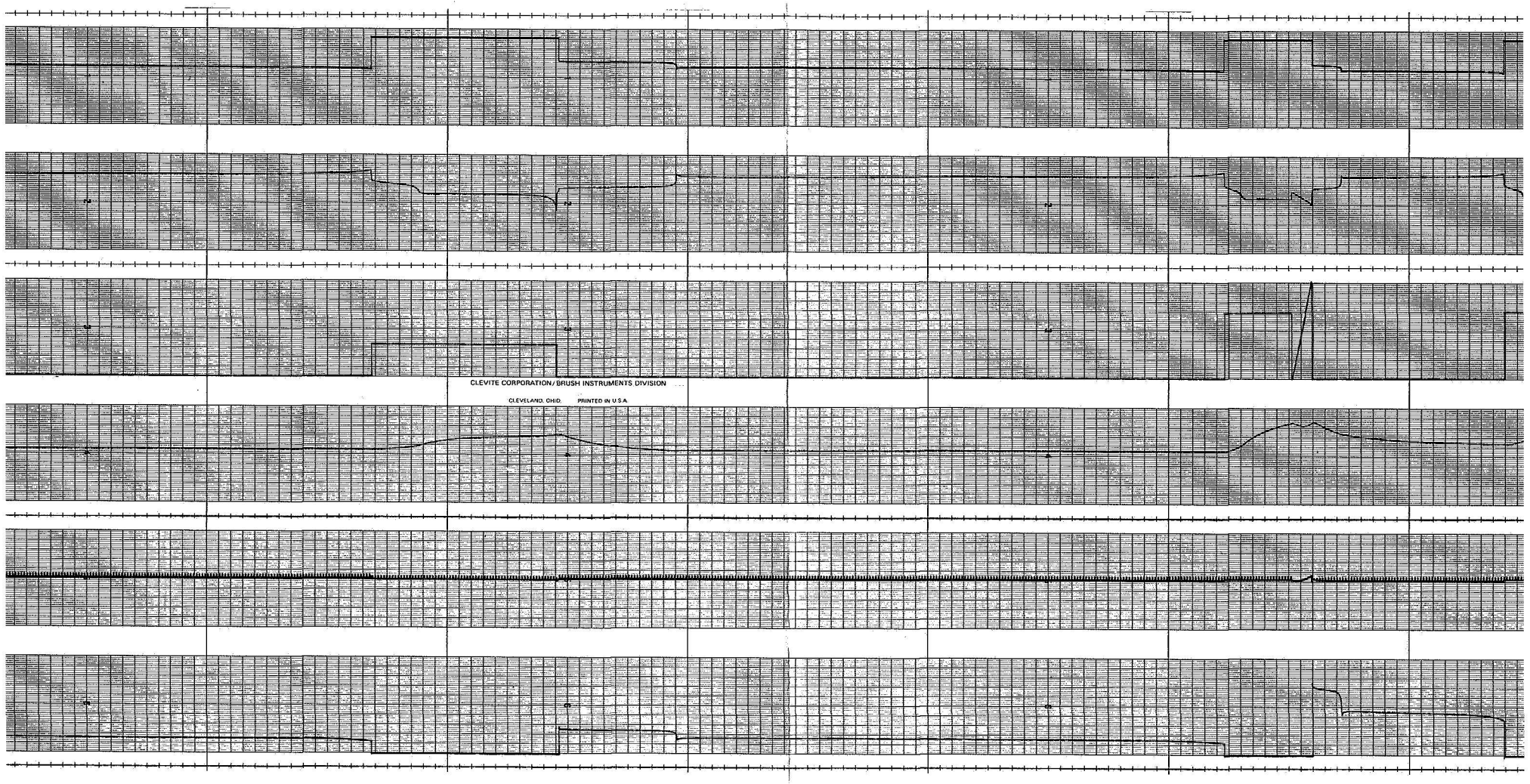

Figure 4. 5a. First Section, Task 3 Test Record, 2nd Test of Cell #20 at 100% DOD

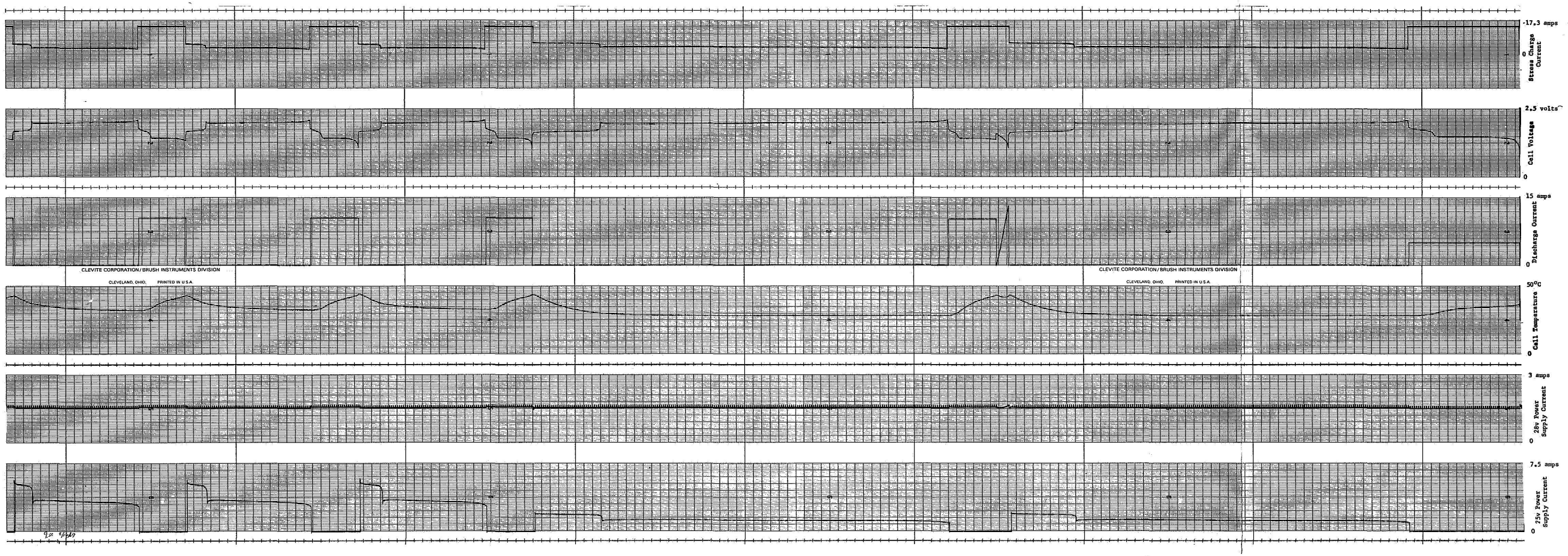

Figure 4. 5b. Second Section, Task 3 Test Record, 2nd Test of Cell #20 at 100% DOD

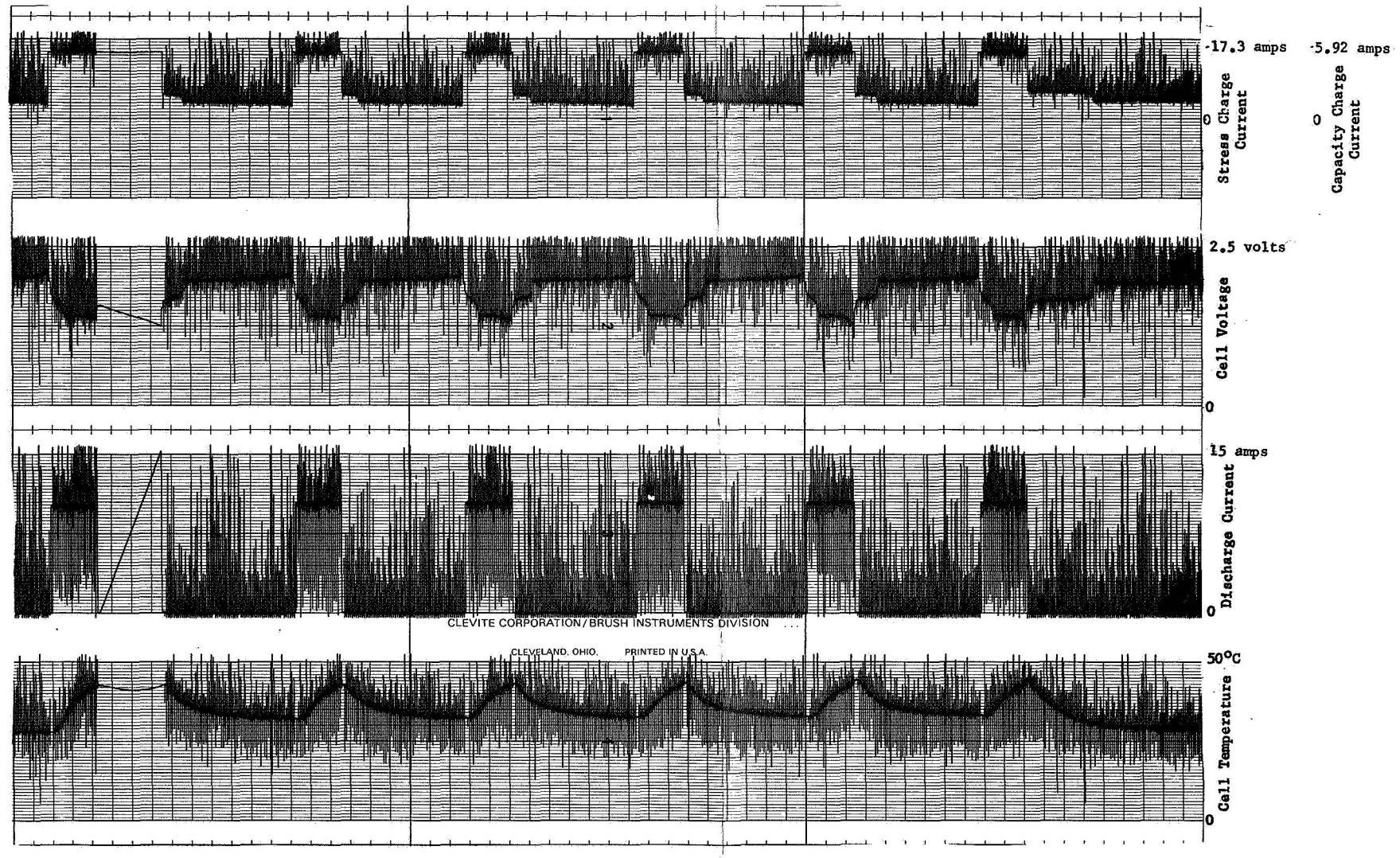

Figure 4.6. Playback of Magnetic Tape Records from Task 3

recorder. This noise can be either positive or negative and, in some cases, both polarities will appear on the reproduced test record. The reproduced test record consists, therefore, of the data plot superimposed on rather large amplitude noise pulses. The noise is inconvenient, but the data can still be read from the chart with good accuracy. Figure 4.6 is a worst case example. Here the noise is exaggerated because of the very slow chart speed employed on playback, and because noise pulses of both polarities are present. However even here, the recorded data is quite legible.

If it were desirable to eliminate the noise pulses, a circuit could be devised that would gate the playback tape recorder output to eliminate the noise excursions. Such a circuit could be designed to eliminate the noise with little loss in data or data accuracy since noise is present for only a very small portion of the 14 sec. data recording interval. Another means of eliminating the noise is to operate the recorder continuously. This presents no problem with the Breadboard Model which has an extremely large tape capacity. This is not a practical approach for the flight version however since there, tape capacity considerations are crucial, and a sampled data operating mode is essential.

4.4. Test Results

The results of the tests are presented below for the cell tests at 65% DOD and three tests at 100% DOD. In addition, results are given for supply voltage sensitivity and temperature sensitivity of certain circuits.

4.4.1 65% DOD

A set of cells was tested with the parameters as listed in Section 4.0. A real time chart record of the test on one of these cells was shown in Figure 4-3. The initial cell capacity was 7.96 amp-hrs. and on the initial polarization, the cell voltage dropped to 1.37 volts when the current was a maximum of 15 amps. After five stress cycles of 65% DOD the measured cell capacity is 7.81 amp-hrs. and during the final polarization the voltage dropped to a low of 1.33 volts. There was almost no cell degradation during this test. The capacity was reduced by about 2% and the voltage during polarization decreased by about 40 mv.

The cell temperature as measured by the thermistor increased during a discharge and decreased toward ambient during a charge. The maximum temperature of 40°C was reached during the polarization when the discharge current was the highest.

The maximum charge current during a capacity charge was 2.1 amps and the average current was about 1.3 amps. The maximum current during a stress charge was 5.1 amps and the average current was about 3.16 amps. The average charge rates during this test were approximately C/4 and C/1.6 for the capacity and stress charges respectively.

4.4.2 100% DOD

A second set of cells was installed and tested using the same parameters except that the stress and polarization discharges were increased to 100% DOD. A chart of this data for Cell #20 is shown in Figure 4-4.

The initial cell capacity was 6.68 amp-hrs. and the cell voltage was reduced to a minimum of 1.36 volt during the first polarization. After five stress cycles at 100% DOD the final cell capacity was the same as the initial or 6.68 amp-hrs. The cell voltage during the final polarization was reduced to 1.30 volts. The cell capacity was not noticeably affected by the high stress rate.

The cell temperature during discharge rose to a maximum of 43.5°C. As before, the maximum temperature occurred during a polarization.

The maximum current during a capacity charge was 2.1 amps and the average current was about 1.3 amp to yield an average charge rate of C/4. The maximum current during a stress charge was 5.4 amps and the average current was about 3.53 amp to yield a charge rate of C/1.4.

The same set of cells was rerun under the same conditions to determine if additional stress cycles would show up signs of cell degradation. A chart of this data for cell #20 is shown in Figure 4-5. The initial cell capacity was measured to be 6.54 amp-hrs. and the cell voltage decreased to 1.26 volts during the initial polarization. The final cell capacity was 5.53 amp-hrs. This is a reduction in cell capacity of some 15.5% during the second set of tests. The polarization voltage decreased to 1.08 volts at a maximum current of 13.2 amp. In this case, the cell voltage was reduced to the low level cut off voltage before the current ramp was complete which results in the polarization test being terminated.

Additional cell degradation is evident when Figures 4-4 and 4-5 are compared. During the stress discharges in Figure 4-4, the cell voltage reached a stable value of about 1.45 volts. During the second set of tests (Figure 4-5) the cell was being discharged nearly to capacity during the stress discharges, and the capacity decreases with subsequent cycles so that the cell voltage becomes lower and lower. The last stress discharge is almost to the point of cutting-off the discharge before the nominal thirty minute period is completed.

This set of cells was run for a third time at 100% DOD. Cell #20 showed an initial capacity of 5.26 amp-hrs. The voltage during polarization was reduced to 1.1 volts with a discharge current of 8.7 amps. After the five stress cycles, the final capacity was 4.84 amp-hrs and is a reduction of 8% during this test. The final polarization voltage was 1.1 volts at a current of 6.3 amps.

The temperature during this period reached 45°C on the case of cell #20. The charge currents were similar to those of the preceeding test. All of the stress cycles during this test were essentially capacity measurements. That is, the cell was completely discharged during each stress cycles and the nominal 30 minute discharge period was reduced to around 20 to 25 minutes.

4.4.3 Supply Voltage Sensitivity Tests

The breadboard circuits were unaffected by ±10% variations of the 28 volt power supply. The 2.5 volt power supply voltage was varied ±10% during a Task 3 test. The only changes that were noticed were variations in the charge current and accompanying variations in charge time. With higher voltage and higher current, the charging time was proportionately less and with lower voltage and current, the time was longer. This was as expected.

4.4.4 Circuit Performance

The overall circuit performance of Task 3 has been good. There were two component failures during Task 3 tests. Specifically, these were the fourth 9301 1-of-10 decoder and the N8162J one-shot multivibrator that provides an end of test output pulse. Any cause for their failure was unapparent and the reason for their failure remains unknown. These failures occurred toward the beginning of the final tests and replacements have operated several weeks with no failure.

4.5 Discussion of Test Results

It is fairly clear that the typical Yardney HR5DC7A cells will not show significant cell degradation during a single run of this test program with a stress discharge of 65%. In fact, a stress cycle with 100% DOD does not show significant degradation during the first test sequence. It is only during the second test sequence at 100% DOD that the cell begins to show signs of degradation but at that, the cell capacity is only reduced from about 135% of rating to 100% of rating.

The polarization voltage is significant from the standpoint that the cell actually polarizes during the second test sequence at 100% DOD. This polarization takes place at a current of between 10 and 15 amps. During the first set of tests at 65% and 100% DOD the cell voltage was reduced during polarization but the cell did not actually polarize.

The maximum temperature that was measured on the outside surface of the cell case was 43°C and was about 18°C above the ambient temperature. The internal cell temperature was no doubt, somewhat higher than this maximum but no measurements were made of the internal temperature.

4.6 Conclusions and Suggestions for Increased Stressing

The Task 3 cells showed little or no degradation during a single test sequence at either 65% DOD or 100% DOD. There are two convenient methods available to increase the stress and increase degradation to a significant level. The first is to cycle the cells more than once at a nominal level of stress. The second is to increase the stress on the cell during a single test by increasing the depth of discharge and recharge rate. The depth of discharge can easily be increased to 200% i.e. 20 amp/.5 hr. and the charge rate can be increased to a maximum of 10 amps. If this is done, the typical cell will be fully discharged during each stress cycle. It must be noted that discharge rates this high would require scale factor changes on the recorders and would require either increased power consumption during charges or longer stress cycles or both. The discharge rate could be increased to 150% i.e. 15a/.5 hr. with no change in scale factor.

The Task 3 logic is designed so that it will make repeated tests of the Task 3 cells automatically. That is, after the sixth cell has been tested to completion, the test will begin again on cell #1. This loop will continue until the tests are terminated manually. The testing sequence is slightly different on the second and subsequent automatic tests. The cells were left uncharged at the end of the first test sequence, therefore, the initial stress discharge will immediately polarize the cells and first capacity charge will recharge the cell. The effect on the cells of this slight change should be insignificant.

5.0 CIRCUIT TEMPERATURE SENSITIVITY

Several selected breadboard circuits were tested for temperature sensitivity over the temperature range from 10^{o} to 50^{o}C. The circuits that were chosen were those that were thought to have the largest temperature effect. These circuits were the voltage level sensors, discharge circuits, relay drivers and clocks.

5.1 Voltage Level Sensor

The voltage level sensor is essentially an extremely high gain amplifier with positive feedback. The amplifier is rated for satisfactory operation over the range from 0^{o} to 70^{o}C. There could be two detrimental effects of temperature on the level sensor circuit. The first would be a change in trigger level with temperature and the second would be a change in the rise time with temperature. If the gain of the amplifier remains high, there should be little temperature effect on the triggering level. Measurements on a typical circuit over the 10 to 50^{o} range show this to be correct. There was no measurable change in the voltage triggering point over the temperature range. This rise time remained fast enough to cause no switching problems.

5.2 Discharge Circuits

The most important discharge circuits from the standpoint of temperature sensitivity is the Task 1 ramp circuit. Measurements were made on the ramp rate over the temperature range from 10 to 50^{o}C. The ramp rate was somewhat temperature sensitive and showed a temperature coefficient of .15%/^{o}C for a 60 ma/min. rate and .32%/^{o}C for a 7 ma/min. rate. This temperature coefficient is acceptable in this application.

5.3 Relay Drivers

Both a normal and a time-delayed relay driver were tested for temperature sensitivity. The output of the driver was connected to a dummy load that could be varied to represent one or more relays in parallel. The worst case minimum relay switching voltage across the load was measured as a function of input voltage at several temperatures over the range. For all loads and temperatures, both relay drivers would guarantee a closed relay at the minimum "1" level and an open relay at the maximum "0" level. A typical set of data is shown in Figure 5-1. Operation in a shaded area indicates faulty operation.

5.4 Clocks

The frequency stability of the clock circuits was measured as a function of temperature. The temperature coefficient was about .1%/^{o}C over the 40^{o} temperature range.

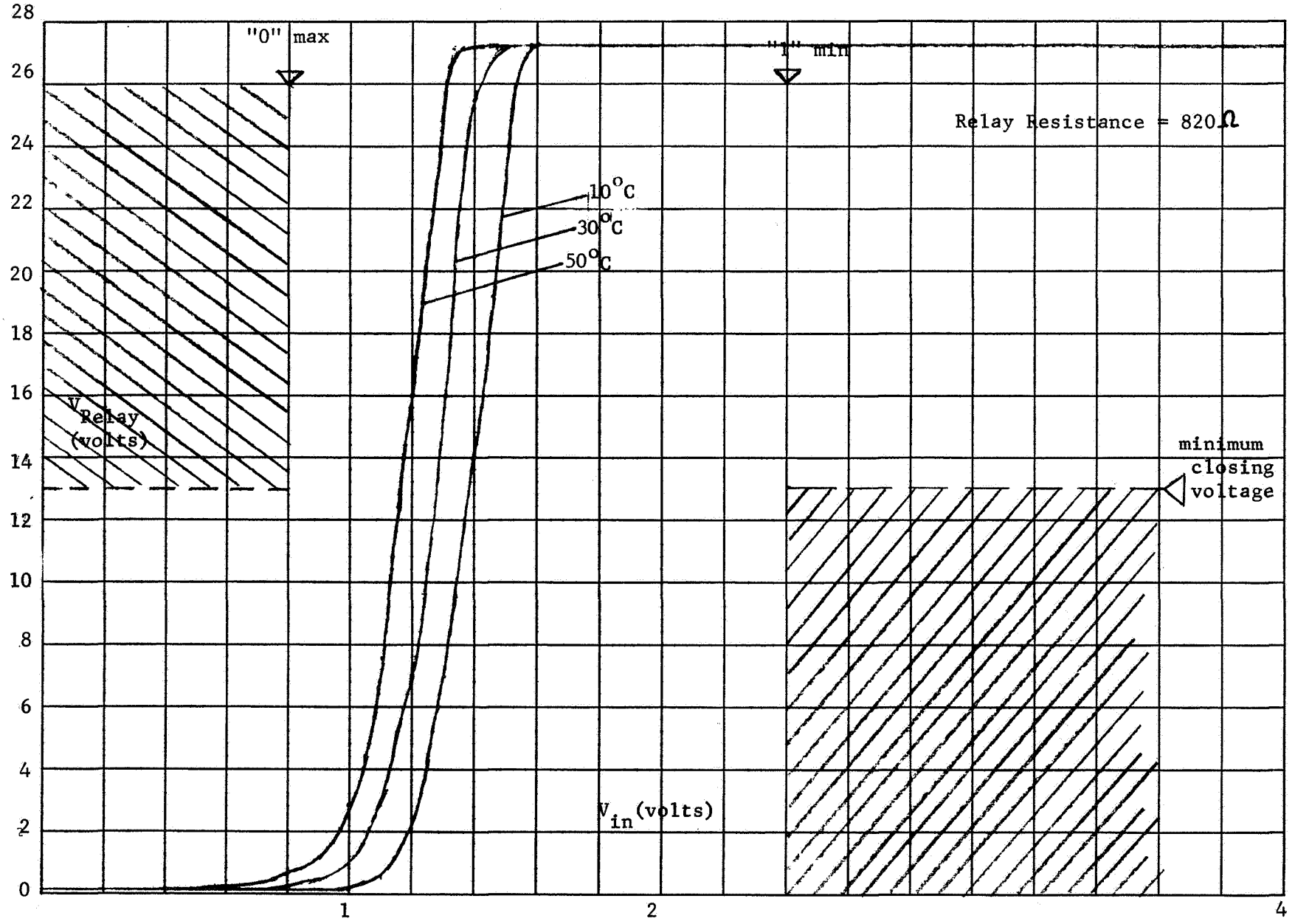
"0" max
"1" min
Relay Resistance = 820Ω
10°C
30°C
50°C
V Relay (volts)
minimum closing voltage
V in (volts)
28
26
24
22
20
18
16
14
12
10
8
6
4
2
0
1
2
4

Figure 5.1

6.0 POWER CONSUMPTION

The power consumption was calculated for each task using the power supply current data that was recorded on Channels 5 and 6 of the chart recorder. Examples are shown in Figure 4-3, 4-4, and 4-5. From these calculations, nine watts should be substracted to obtain the instrument power consumption. The nine watts is the power drawn by the recorder solenoids and would not be necessary on a subsequent flight version. The maximum and average power consumption figures are given in Table 6.1 for all three tasks.

Table 6.1 Power Consumption

	Task 1	Task 2	Task 3 (100% DOD)
Maximum:	26.8	49.7	49
Average:	26.8	46.4	39

7.0 FLIGHT VERSION CONSIDERATIONS

The breadboard circuitry was designed to make use of types of components that would have an excellent chance of becoming flight qualified. In general, the breadboard was constructed using devices that followed this philosophy. For many devices, such as relays, capacitors, resistors, and some integrated circuits flight qualified versions are available.

Estimates have been made of the weight, size, and power consumption that might be expected of a future flight version. These are a weight of 60 lbs., a size of 6 $ft.^3$ and an average consumption of 45 watts.

8.0 CONCLUSIONS

From the experimental results obtained to date it is possible to draw a number of conclusions concerning the adequacy of the various task experiments and their equipment implementations. These are as follows.

8.1 Task I Experiment

The current ramp approach employed here has proved to be a readily achieveable and very reproducible test method. The results obtained with it can be directly correlated with previous results obtained by JPL at one gravity, provided an adequate allowance is made for the depth of discharge achieved in the test. Expectations that depth of discharge was a significant parameter with a primary effect on test results have been borne out in the experimental results obtained. This has pointed out the essential need to maintain equivalent DOD values in tests designed to establish sensitivity to other effects such as gravity. The method employed in Task I to control depth of discharge, viz. by controlling the current ramp rate, has proved to be a simple and effective approach to solving this problem. The ability to simulate 0-g on the Task I cells by suitably orienting the electrode so that convection effects are minimized provides a convenient means of assessing the significance of gravity dependent effects.

Additionally, it provides a convenient method for prelaunch checkout of the equipment for this experiment in a way which more nearly approximates behavior which should occur with 0-g.

In the tests of the Task 1 experiment conducted to date, the activation sequence has been found to be simple, effective, and trouble free; and the venting arrangement and vent trap system appear to be fully adequate. The

cell design evolved has proven to be adequately leak tight for the application, and permits changing of the test electrode to be done easily. In view of the repeatability of the results obtained to date, it appears that a sample size of six should be fully adequate in this type of test.

In general, we believe that the Task 1 test as implemented could be readily carried out in a flight experiment, and therefore, should serve as a sound basis for the design of equipment for flight use.

8.2 Task 2 Experiment

Before the Task 2 experiment can be conducted at 0-g conditions it is quite evident that further development of the experimental approach and its implementation will be necessary.

In particular, the gas management system associated with the special cells of Task 2 has proven to be marginal at best, and under conditions where gassing in the cells is emphasized, the gas separation sometimes fails completely. The primary problem here apperars to be the high efficiency of the centrifugal pump as a gas separator. This tends to trap gas in a part of the system where it can not be tolerated during subsequent evacuation cycles.

Another problem is the discrepancy between the surplus discharge capacity values measured in tests carried out according to the procedure described in the Test Plan, and those found in prior bench top tests. This raises questions concerning the optimum value of certain parameters which are controlled in the test sequence and electrode structure imperfections.

To clarify these questions it will be necessary to do considerably more testing of the Task 2 test sequence using various values of test parameters such as initial charge current and discharge current density, while controlling the

degree of imperfection of the test electrode assembly. This should result in more closely defined values of those parameters selected to enhance the cell sensitivity to gas loading, and permit a more optimum setting of parameter values in the automatic cell tests.

Results to date point up the need for certain revisions in the Task 2 cell design to reduce the tendency to trap gas in front of the test electrode even when the recirculating system is functioning normally. This occurs primarily in the inverted cone structure which supports the auxiliary electrode in the cell. Consideration should be given to repositioning this support or redesigning it to eliminate gas trapping, and possibly increasing circulation rate.

Another factor which should be considered in any cell redesign is gas leakage under vacuum. Emphasis on achieving a design which minimizes sources of leakage is essential. This has been pointed out by the numerous instances where significant leakage has occurred during the testing program. Such leakage becomes very apparent during the electrolyte filling operation while the cell is maintained under vacuum conditions. In many instances it has been possible to make temporary repairs to reduce the leakage to tolerable values, but this approach would not be acceptable for a flight unit. Also the situation will be greatly aggravated when cells are subjected to vibration during launch. Thus it appears that a minimization of the number of seals involved is essential, and greater attention must be given to seals where leads emerge from the cell.

In the case of the silver test electrode, difficulties has been encountered due to the Cellophane separator darkening which obscures the view of

gas accumulation on the silver electrode surface. This is evidently due to a reaction between the silver ion in solution and the Cellophane. To eliminate this problem an investigation of alternate separator materials should be carried out.

In general, it appears that further development and test refinement is necessary before a form of the Task 2 experiment will be ready for flight use under 0-g conditions. We believe that most of the changes necessary to make this experiment workable involve the hardware for the gas and electrolyte handling systems. The logic and control as implemented will probably require but little change. The photographic approach used has proven to be satisfactory except for the problem encountered with separator darkening in the case of the silver cell.

The measurements of a high current density residual discharge capacity of commercial electrode systems or batteries as a function of trapped gas removal by evacuation may turn out to be a convenient tool for determining the degree of gas trapping in such systems. The verification of such correlations is recommended.

8.3 Task 3 Cells

The Task 3 experiment as implemented fulfills all the requirements set forth in the Test Plan. In many respects, it goes beyond the requirements indicated because it became apparent as test data accumulated that versatility would be useful in establishing a test program which gave a reasonable degree of degradation for this type of battery. Whereas the Test Plan stipulates a maximum depth of discharge of 75%, the equipment is capable of providing a 100% depth of discharge in a 30 minute time interval, proven by the con-

siderable testing done at this level.

It appears that the main problem in conducting the Task 3 experiment is to establish a test regime which gives an adequate amount of degradation. Whereas, originally, advice from the battery manufacturer and other expert opinion indicated that 65% depth of discharge would be more than adequate to cause degradation, this has not been found to be the case. A negligible amount of capacity loss has been measured even when the cells are discharged to 100% depth of discharge in 30 minutes. In most cases, such cells even after the second Task 3 test sequence show low degradation. Thus, it appears that more than 5 stress cycles will be necessary, and probably these will have to be conducted to a greater depth of discharge to show up a significant loss in battery capacity.

There is no reason why more extended tests of the Task 3 type cannot be conducted with the equipment as it stands. Provision has been included so that the Task 3 test recycles once the test of the 6th cell has been completed. This will permit accumulation of information on the number of stress cycles required to cause degradation with various stress levels applied. More information from such tests would appear to be essential in order to provide a more specific test sequence for the Task 3 experiments. Once such a test sequence is defined the necessary modifications could be incorporated to adapt the system to that type of test. Probably the main limitation in longer test sequences will be additional capacity required of the tape recorder in the system.

In its present form the Task 3 experiment implementation provides a convenient way of acquiring experimental data on silver zinc commercial cells

over a limited range of sizes. It provides the basic design philosphy which could be followed with minimum change in adapting this experiment for use in space. Of the three tasks, it has been tested more extensively than any of the others. There has been a minimum of problems during such tests and operation has been consistent and reliable.

8.4 General

The solid state logic and control system for all three experiments has been proven as a reliable and trouble free method of carrying out this type of test. It provides a system which is insensitive to expected variations in supply voltage and ambient temperature, and maintains power consumption within the limits set in the initial contract definition.

Tested most extensively in the Task 3 experiments, operation has been quite reliable during 750 hours operating time to date. The very few component failures noted would probably ordinarily be eliminated had any component burn-in cycle been followed.

Because of the length of time involved in carrying out the Task 3 experiment it was necessary to utilize a recording method with high tape efficiently. The sampled method employed in the equipment has proven to be effective and reliable. Playback at fast tape speeds of such sampled records has proved to be a convenient and simple way of reducing the data.

Power measurements made throughout all of the three experiments have shown that less than 50 watts total average power is required to carry out the test series.

In general it appears that the breadboard model represents a realistic approach to carrying out this type of experiment and particularly in the case

of Task 1 and 3 experiments. A minimum of change should be necessary to preapre these experiments for operation under 0-g conditions. In the case of Task 2, the control logic has been proven to fulfill the requirements set forth in the Test Plan. However, problems with gas management and controlled electrode imperfections in the Task 2 experiment will necessitate further development.

If flight schedules do not permit such additional development, it may be advisable to include only the Task 1 and Task 3 experiments in the first flight tests. Then results from these first tests could be factored into any decision on what should be done in the Task 2 area. For example, if it could be established that 0-gravity had no significant effect on the capacity of commercial cells, the necessity of carrying out the Task 2 experiment would be avoided. On the other hand, if significant loss in capacity of commercial cells were found in the 0-g experiment, then the Task 2 experiment probably would be of considerable value, and perhaps one might wish to expand it to study in more detail the other effects which could contribute to loss of capacity under 0-g conditions.

9.0 NEW TECHNOLOGY

There are no "New Technology" items reportable from this Research and Development effort.